

Supporting Information

The rare example of compact heteroleptic cyclometalated iridium(III) complexes demonstrating well-separated dual emission

Anastasia Yu. Gitlina,^a Maria V. Ivonina,^a Vladimir V. Sizov,^a Galina L. Starova,^a Anatoly P. Pushkarev,^b Dmytro Volyniuk,^c Sergey P. Tunik,^a Igor O. Koshevoy^d and Elena V. Grachova^{a*}

^a St. Petersburg State University, Institute of Chemistry, Universitetskii pr. 26, 198504 St. Petersburg, Russia

^b Department of Nanophotonics and Metamaterials, ITMO University, 197101 St. Petersburg, Russia

^c Department of Polymer Chemistry and Technology, Kaunas University of Technology, 50254 Kaunas, Lithuania

^d University of Eastern Finland, Department of Chemistry, 80101 Joensuu, Finland

Content

Table S1. Crystal data and structure refinement for **1-3**.

Figure S1. ESI⁺ MS of complexes **1-5**.

Figure S2. ¹H and ¹H¹H COSY NMR spectra of **epbpy**.

Figure S3. ¹H and ¹H¹H COSY NMR spectra of **1**.

Figure S4. ¹H and ¹H¹H COSY NMR spectra of **2**.

Figure S5. ¹H and ¹H¹H COSY NMR spectra of **3**.

Figure S6. ¹H and ¹H¹H COSY NMR spectra of **4**.

Figure S7. ¹H and ¹H¹H COSY NMR spectra of **5**.

Figure S8. TG/DTG for the complexes **1-5** in argon atmosphere.

Figure S9. Absorption, excitation, and emission spectra of free **epbpy**.

Figure S10. Emission spectra of degassed solution of **1-5** and the photo of degassed and aerated solution of **1**.

Figure S11. Low energy part of **1-5** emission spectra (**PH** band) for time-resolved experiments and relaxation curves for different wavelengths in solution.

Table S2. Photophysical properties of the complexes **1-5** in the solid state at variable temperature.

Table S3. Summary of emission energy maxima for **1-5** in different media.

Figure S12. Solid state emission spectra of **1-5** at variable temperature.

Figure S13. Solid state relaxation curves at variable temperature.

Figure S14. Normalized excitation and normalized on **PH** band emission spectra of **1-5**.

Figure S15. **FL** excitation and **FL** part of emission spectra of **1-5**.

Selection of computational methodology

Figure S16. Comparison of pure DFT functionals PBE and TPSS.

Figure S17. Comparison of hybrid DFT functionals PBE0, TPSSh and CAM-B3LYP.

Table S4. Experimental and computed bonds length (Å) and angles (°) of **1-5**.

Figure S18. Computed UV-vis spectra of **1-5** in solution.

Figure S19. Visualization of triplet transitions in **1-5** by NTO.

Figure S20. Energies of low-lying singlet and triplet excited states obtained from TDDFT calculations for **1-5**.

Table S5. Natural Transition Orbital analysis of electronic excited states in **1-5**.

Table S1. Crystal data and structure refinement for **1-3**.

Compound	1	2	3
Empirical formula	C ₄₀ H ₂₈ IrN ₄ F ₆ P×CH ₂ Cl ₂	C ₄₂ H ₃₂ IrN ₄ ×CH ₂ Cl ₂ ×F ₆ P	C ₅₂ H ₃₆ IrN ₄ O ₄ ×F ₆ P×0.75(CH ₂ Cl ₂)×0.5(C ₄ H ₈ O ₂)
Formula weight	986.76	1014.81	1225.76
Temperature/K	100(2)	100(2)	200(2)
Crystal system	monoclinic	triclinic	triclinic
Space group	P2 ₁ /c	P-1	P-1
a/Å	18.8332(3)	9.7209(4)	12.8631(3)
b/Å	37.4125(5)	11.7561(4)	14.9901(4)
c/Å	10.84780(14)	18.1069(7)	16.3368(3)
α/°	90	92.843(3)	110.0183(19)
β/°	98.0557(13)	96.989(4)	99.1822(17)
γ/°	90	109.734(4)	100.8218(19)
Volume/Å ³	7567.91(17)	1924.14(14)	2820.27(11)
Z	8	2	2
ρ _{calc} /mg/mm ³	1.732	1.752	1.443
m/mm ⁻¹	9.106	3.718	6.084
F(000)	3872.0	1000.0	1219.0
Crystal size/mm ³	0.22 × 0.16 × 0.10	0.34 × 0.22 × 0.10	0.34 × 0.22 × 0.08
Radiation	CuKα (λ = 1.54184)	MoKα (λ = 0.71073)	CuKα (λ = 1.54184)
2θ range for data collection	6.694 to 140	5.582 to 54.998	8.156 to 139.998
Index ranges	-16 ≤ h ≤ 22, -41 ≤ k ≤ 45, -13 ≤ l ≤ 11	-11 ≤ h ≤ 12, -15 ≤ k ≤ 15, -23 ≤ l ≤ 17	-15 ≤ h ≤ 15, -18 ≤ k ≤ 18, -19 ≤ l ≤ 19
Reflections collected	29043	19047	57831
Independent reflections	14068 [R _{int} = 0.0532, R _{sigma} = 0.0556]	8830 [R _{int} = 0.0800, R _{sigma} = 0.1079]	10598 [R _{int} = 0.0856, R _{sigma} = 0.0461]
Data/restraints/parameters	14068/37/991	8830/2/534	10598/0/698
Goodness-of-fit on F ²	1.047	1.051	1.046
Final R indexes [I ≥ 2σ (I)]	R ₁ = 0.0581, wR ₂ = 0.1416	R ₁ = 0.0533, wR ₂ = 0.1029	R ₁ = 0.0492, wR ₂ = 0.1253
Final R indexes [all data]	R ₁ = 0.0708, wR ₂ = 0.1516	R ₁ = 0.0703, wR ₂ = 0.1132	R ₁ = 0.0538, wR ₂ = 0.1307
Largest diff. peak/hole / e Å ⁻³	3.75/-2.25	2.51/-2.52	1.65/-2.57
CCDC numbers	1578517	1539312	1538647

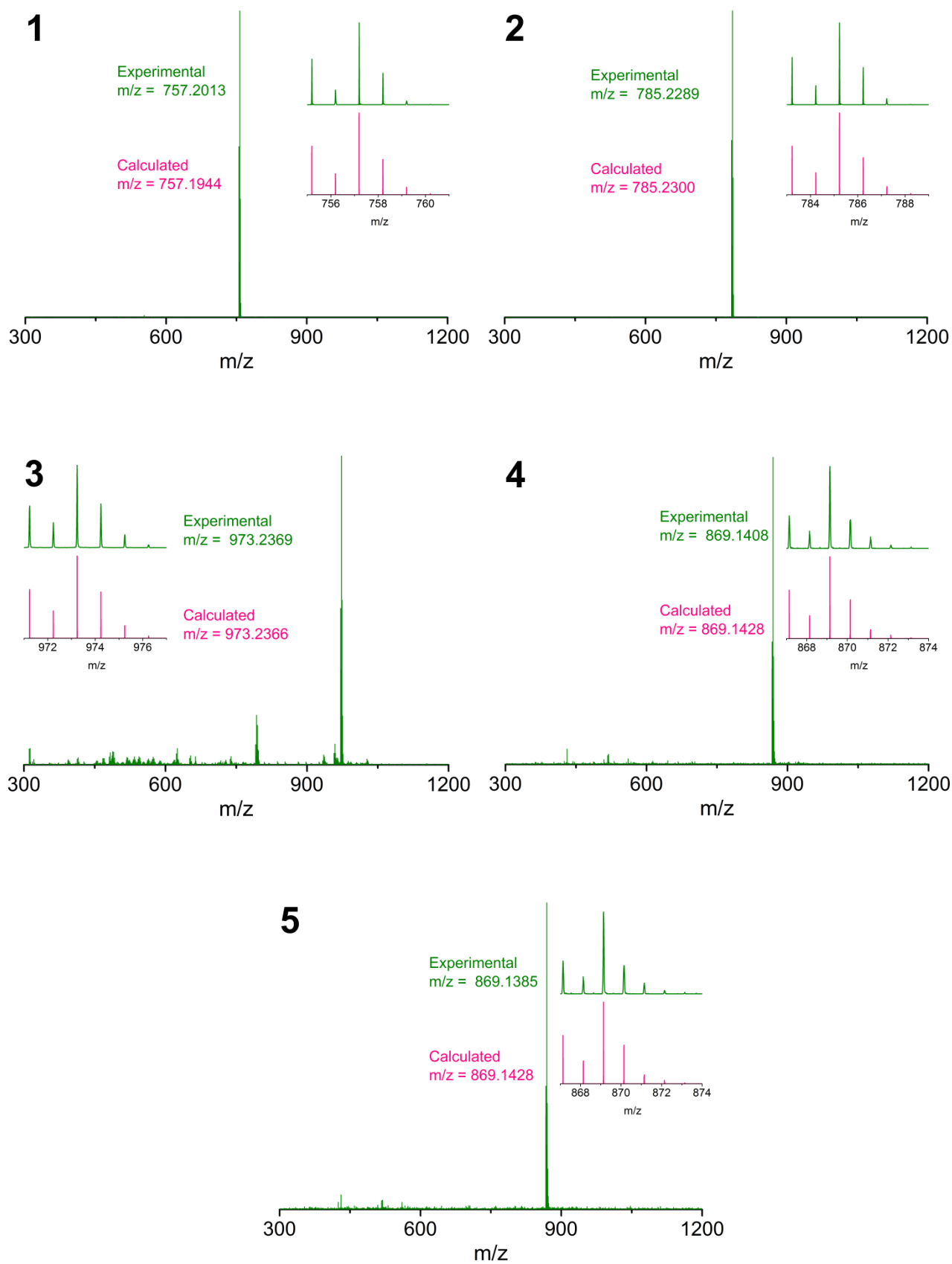


Figure S1. ESI⁺ MS of complexes **1-5**; calculated and experimental m/z are given for the peak with maximum intensity.

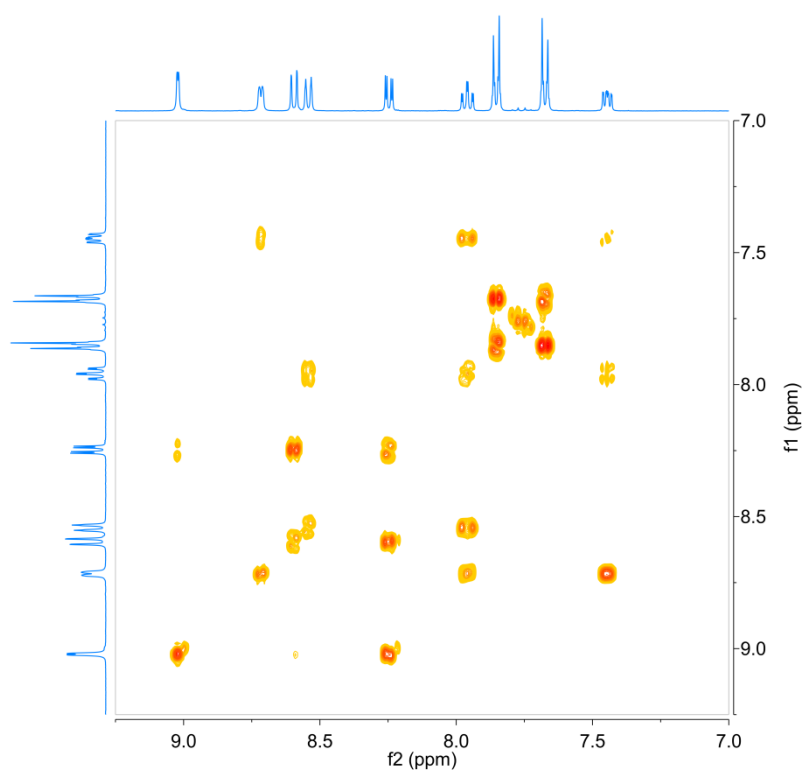
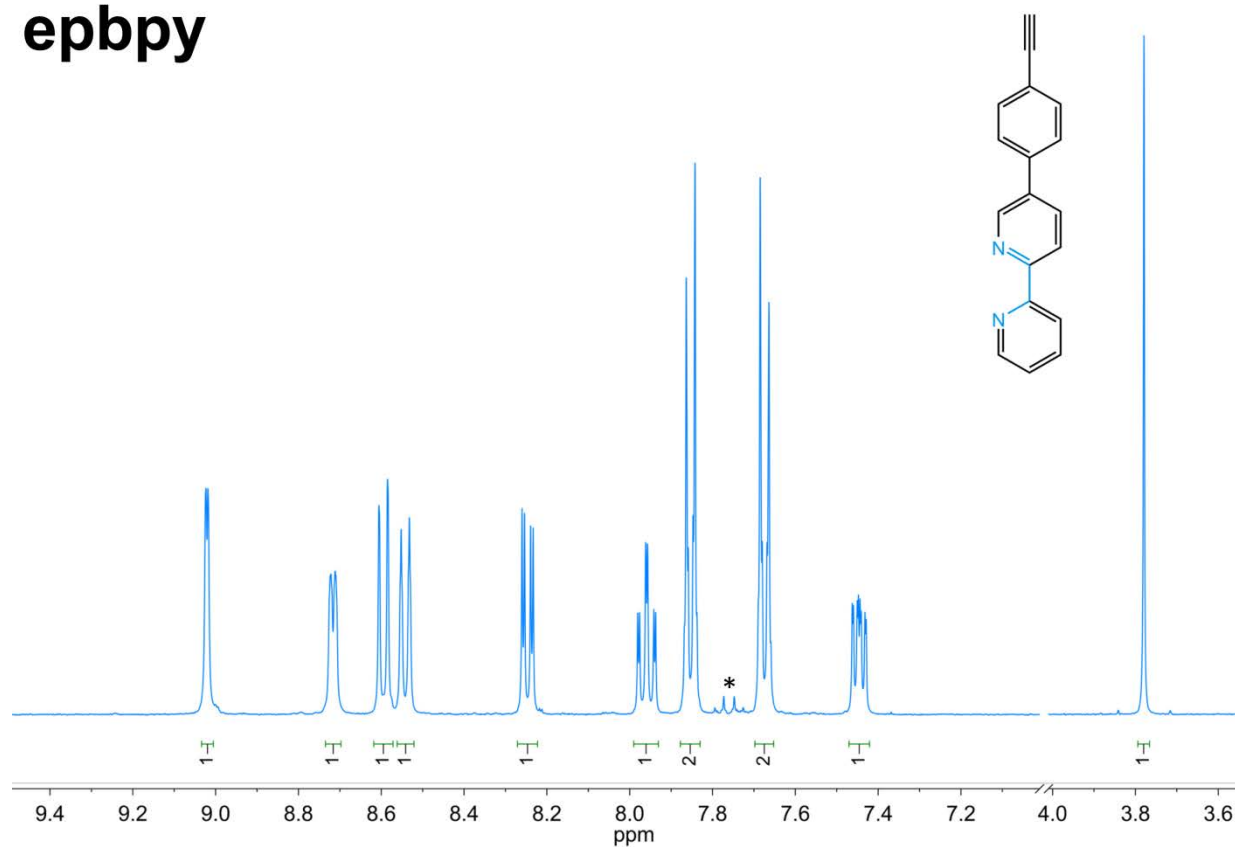
epbpy

Figure S2. Top: ^1H NMR spectra of **epbpy** (acetone- d_6 , r.t., aromatic range). Bottom: ^1H - ^1H COSY NMR spectrum of **epbpy** (acetone- d_6 , r.t., aromatic range). An admixture from the solvent is marked by asterisk.

1

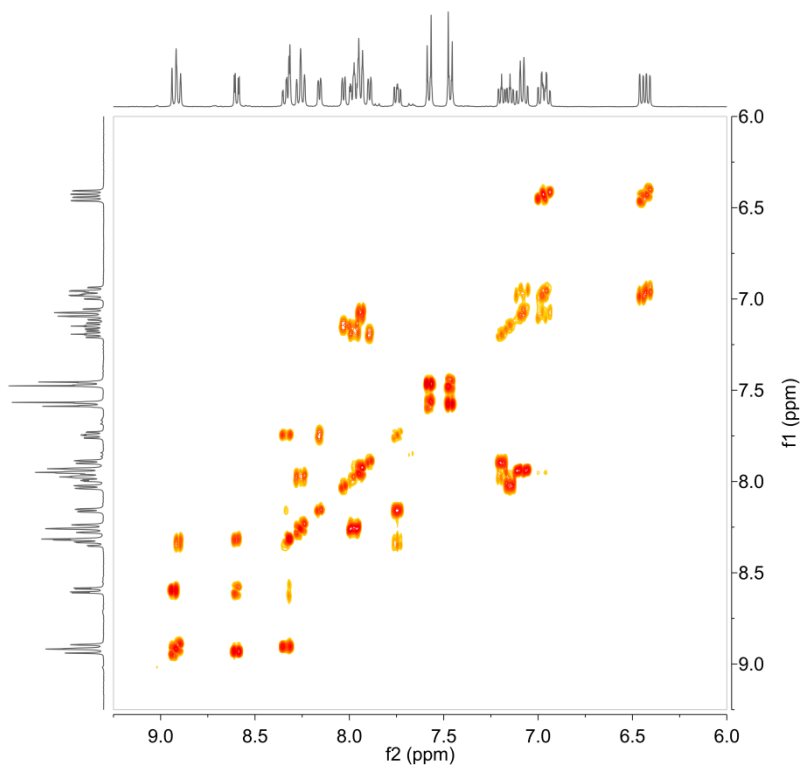
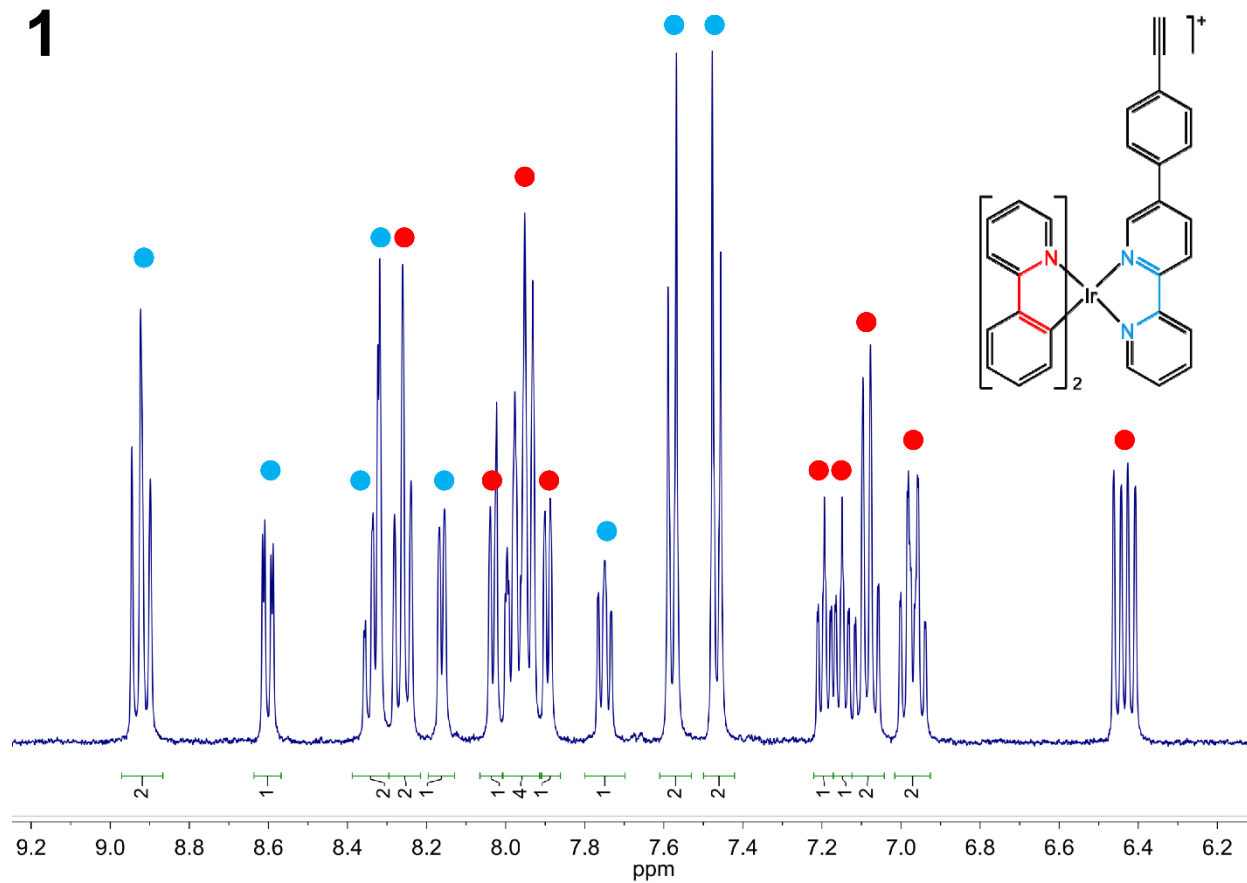


Figure S3. Top: ^1H NMR spectra of **1** (acetone- d_6 , r.t., aromatic range). Bottom: ^1H - ^1H COSY NMR spectrum of **1** (acetone- d_6 , r.t., aromatic range).

2

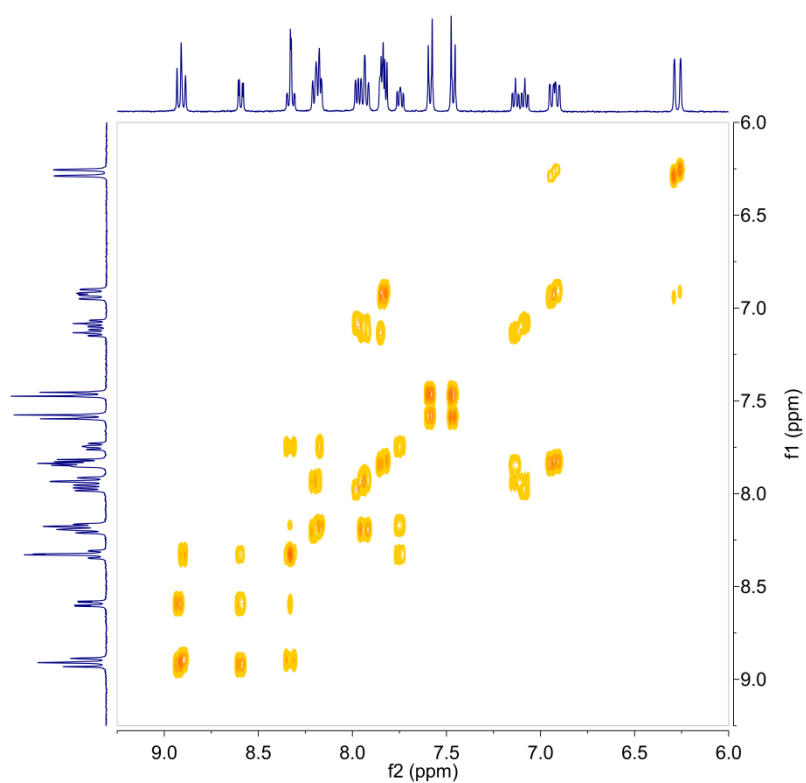
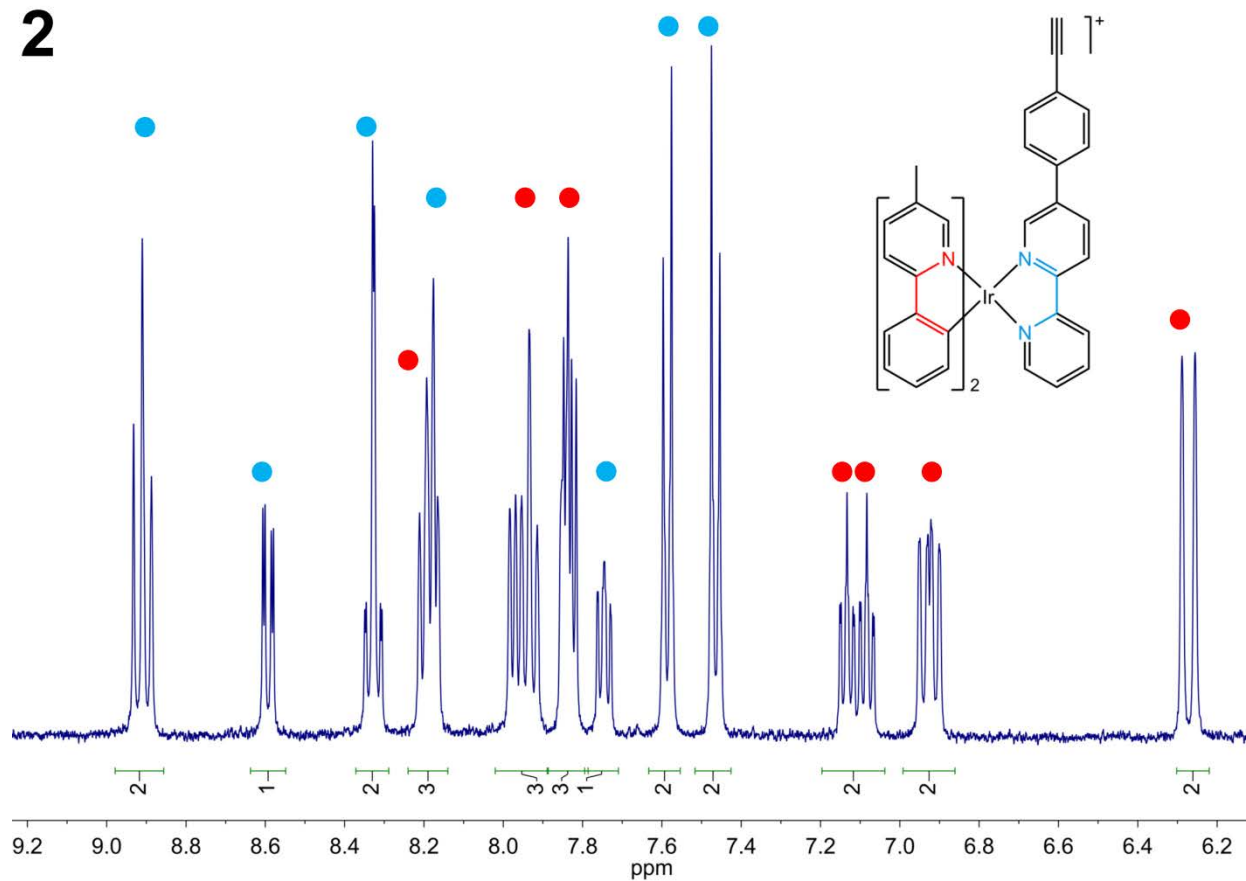


Figure S4. Top: ^1H NMR spectra of **2** (acetone- d_6 , r.t., aromatic range). Bottom: ^1H - ^1H COSY NMR spectrum of **2** (acetone- d_6 , r.t., aromatic range).

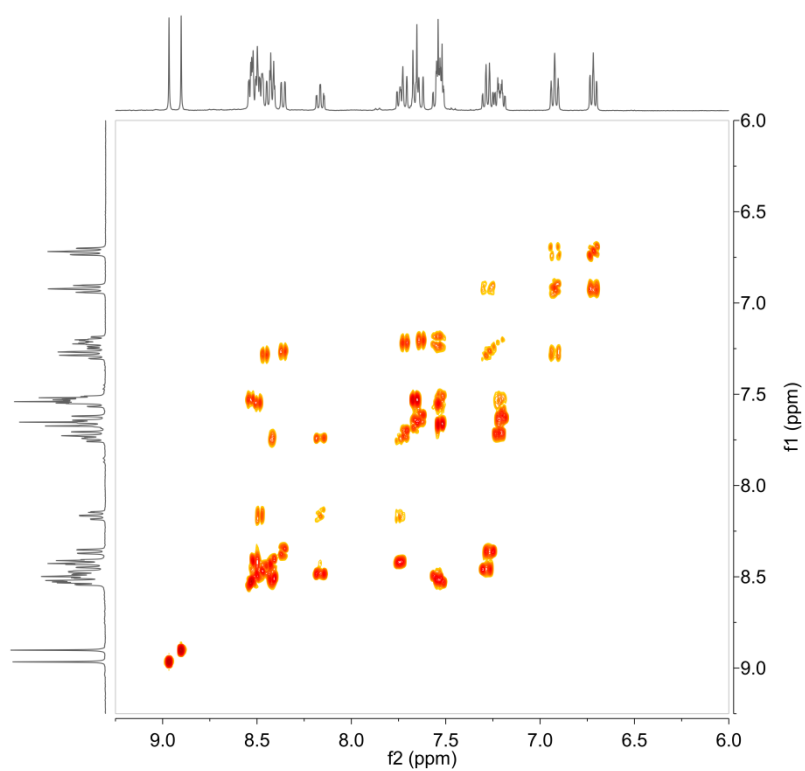
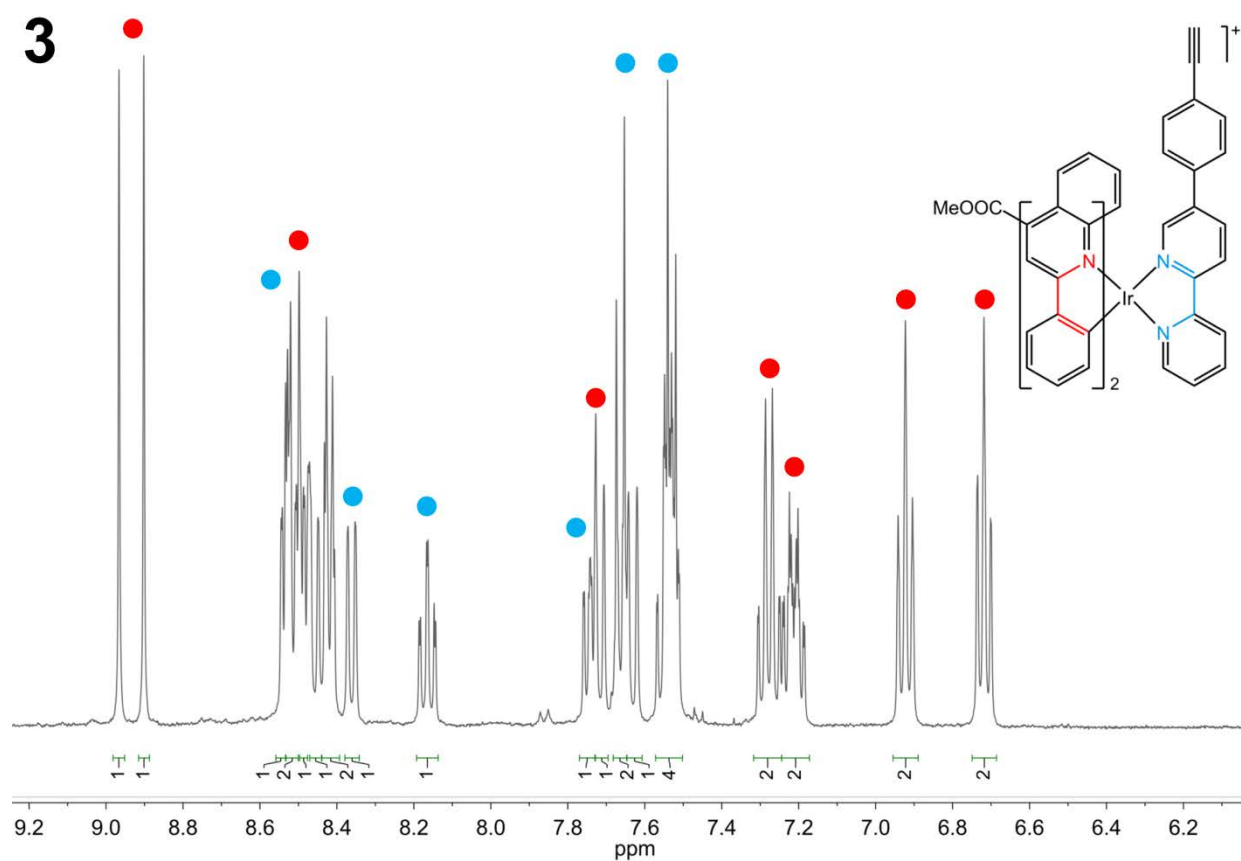


Figure S5. Top: ^1H NMR spectra of **3** (acetone- d_6 , r.t., aromatic range). Bottom: ^1H ^1H COSY NMR spectrum of **3** (acetone- d_6 , r.t., aromatic range).

4

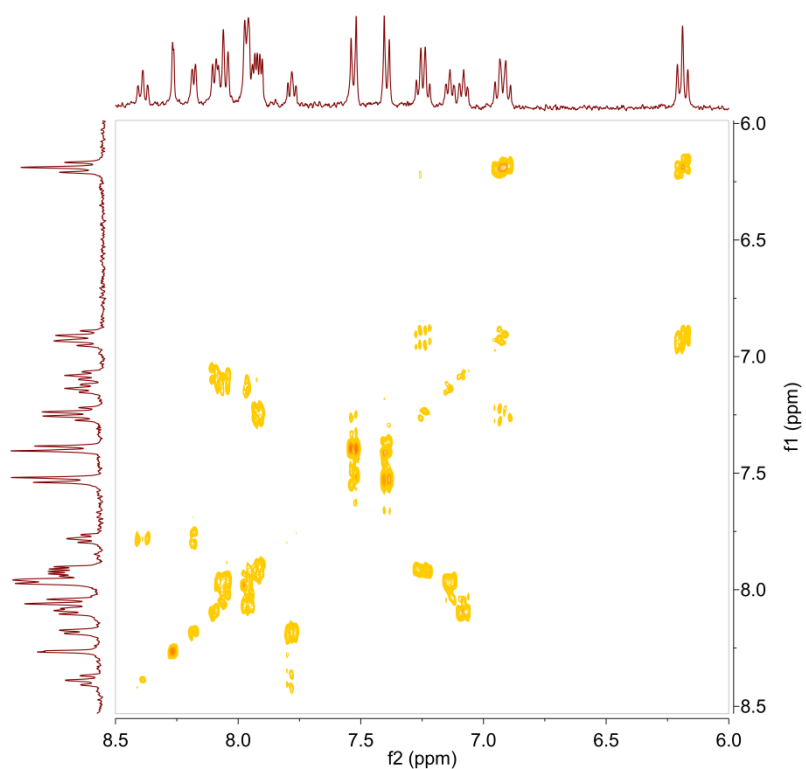
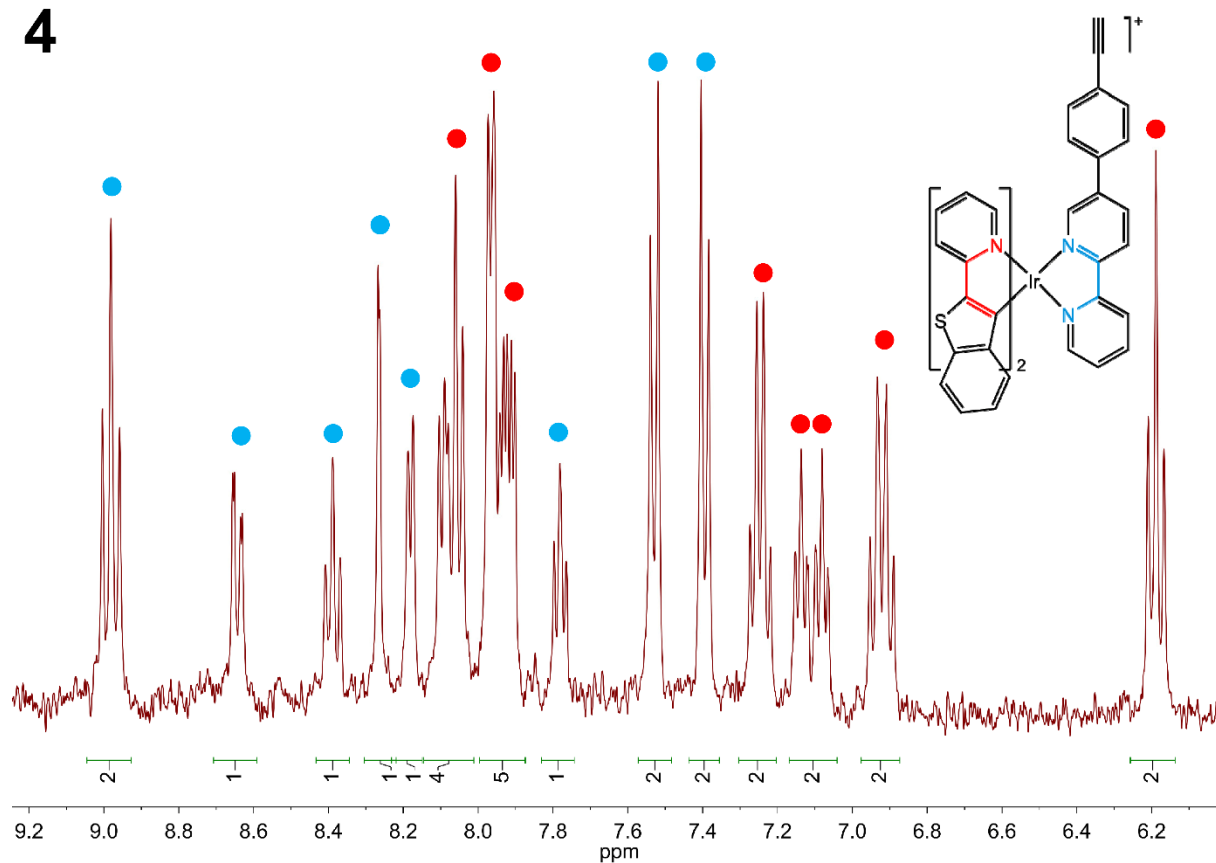


Figure S6. Top: ^1H NMR spectra of **4** (acetone- d_6 , r.t., aromatic range). Bottom: ^1H ^1H COSY NMR spectrum of **4** (acetone- d_6 , r.t., aromatic range).

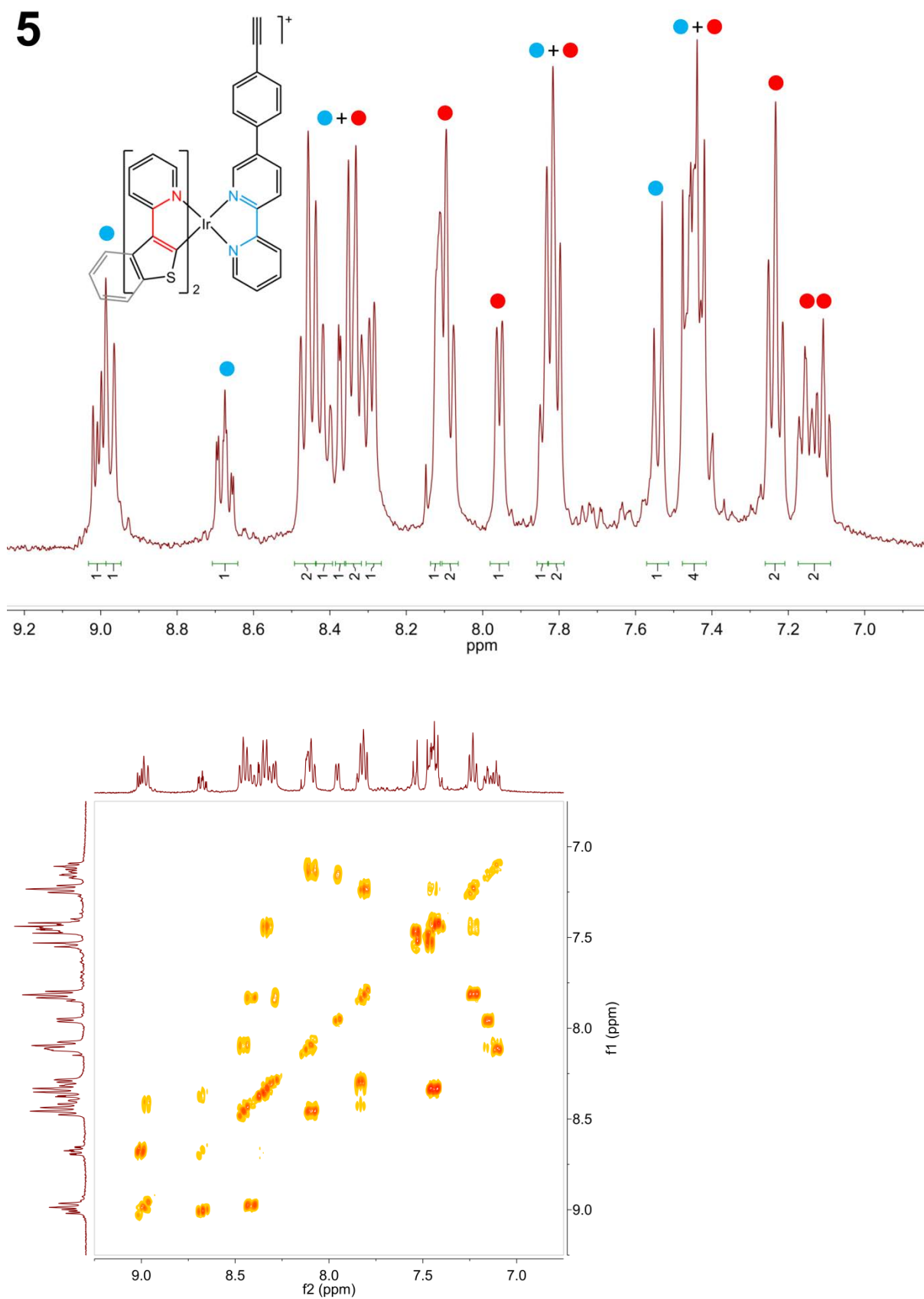
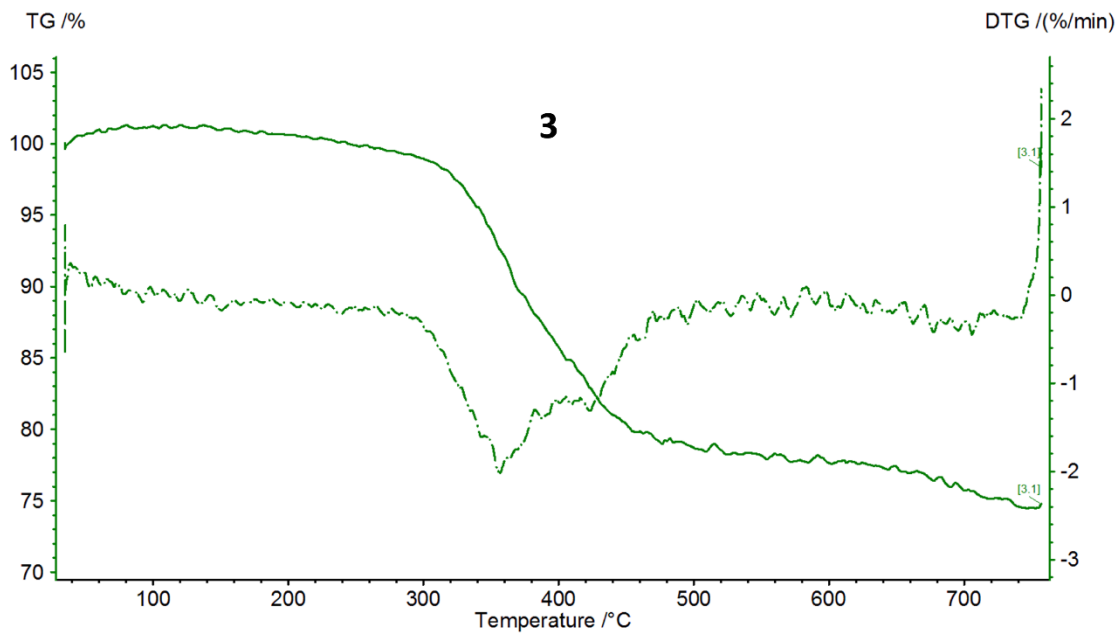
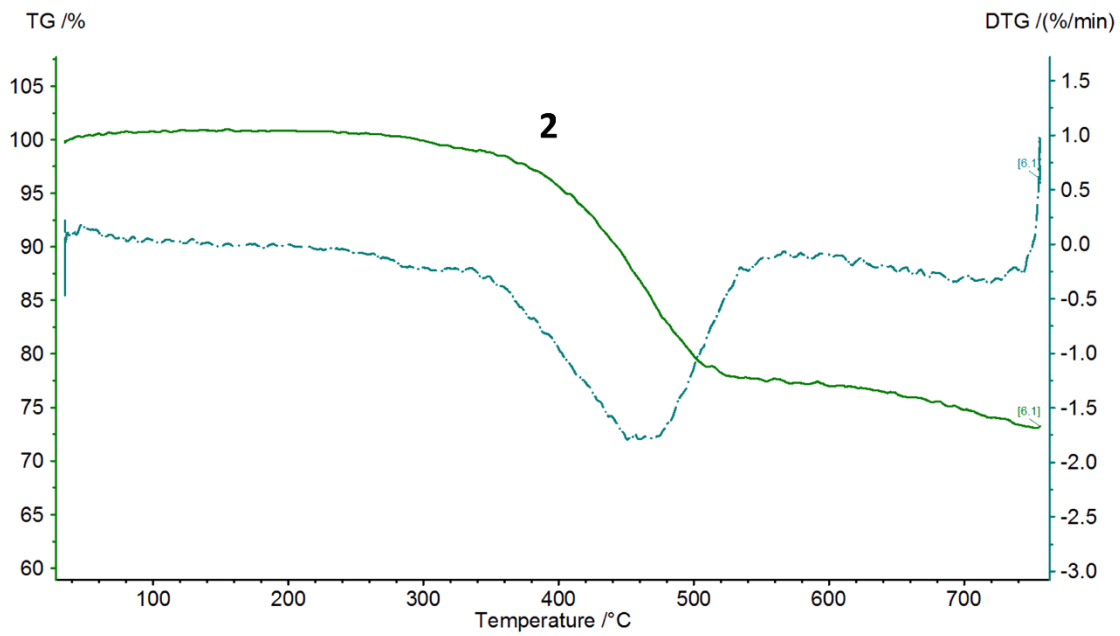
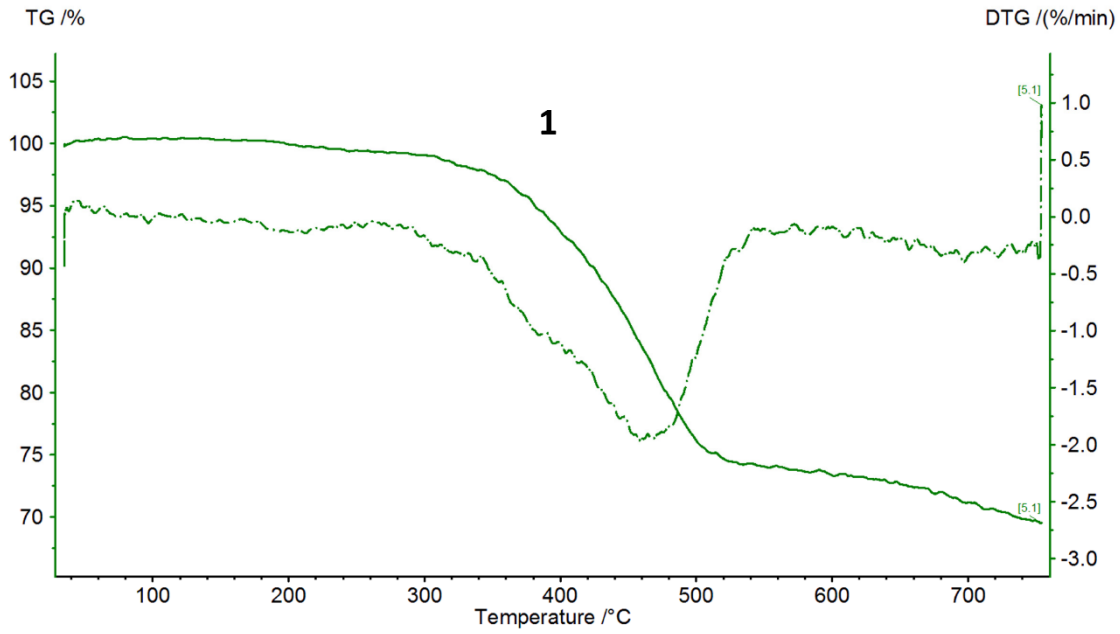


Figure S7. Top: ^1H NMR spectra of **5** (acetone- d_6 , r.t., aromatic range). Bottom: ^1H ^1H COSY NMR spectrum of **5** (acetone- d_6 , r.t., aromatic range).



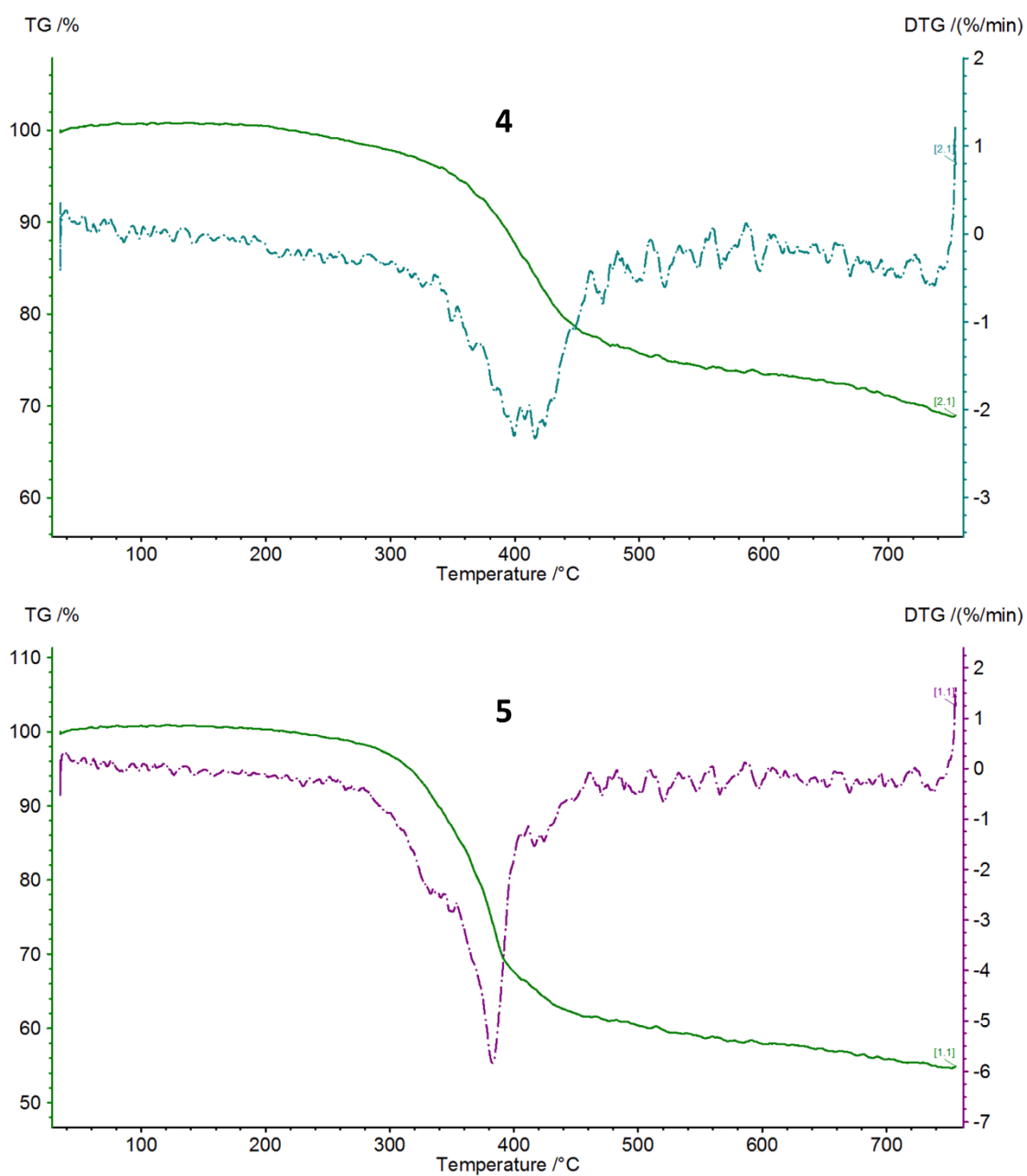


Figure S8. TG/DTG for the complexes **1-5** in argon atmosphere.

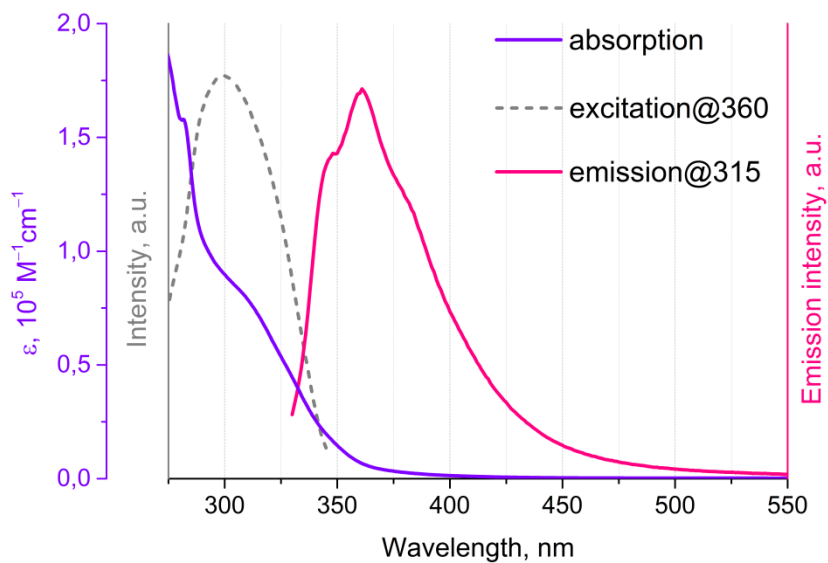


Figure S9. Absorption, excitation, and emission spectra of free **epbpy** (1,2-dichloroethane solution, r.t.).

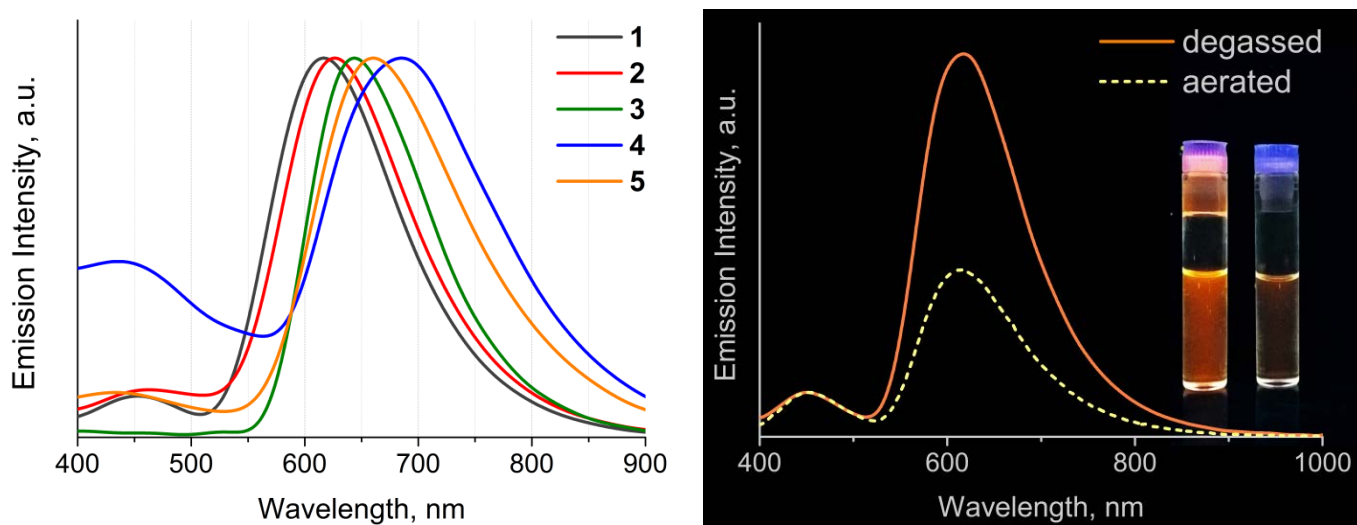
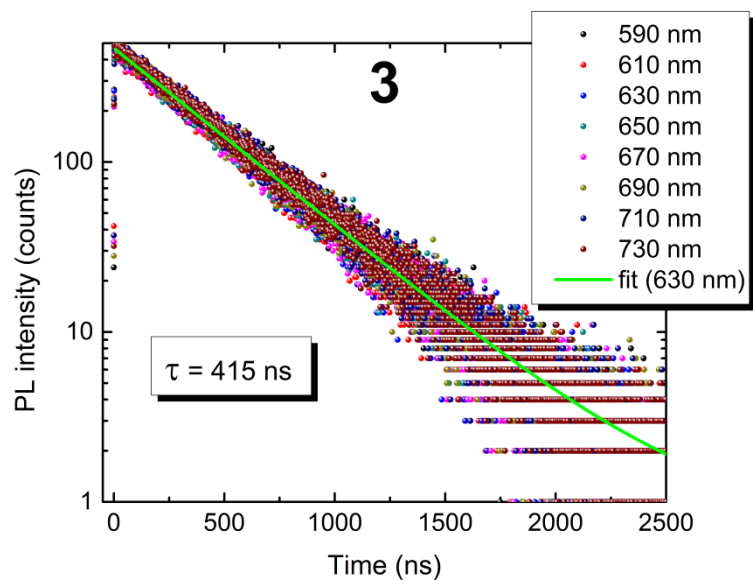
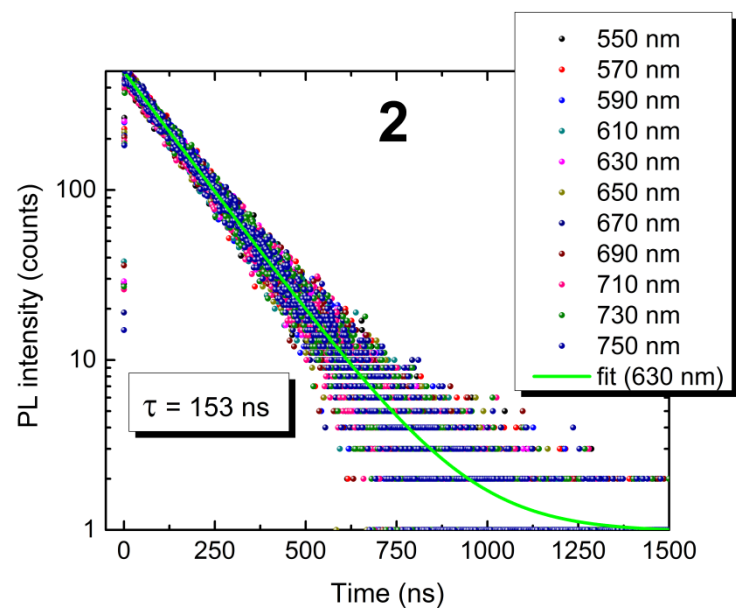
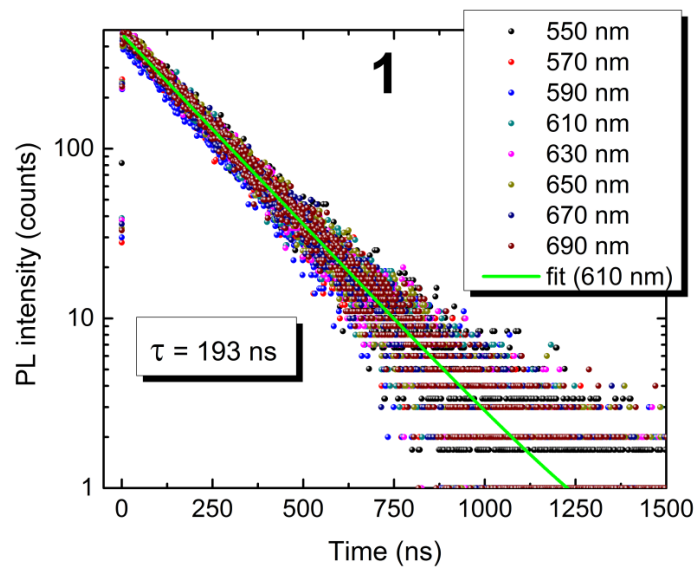
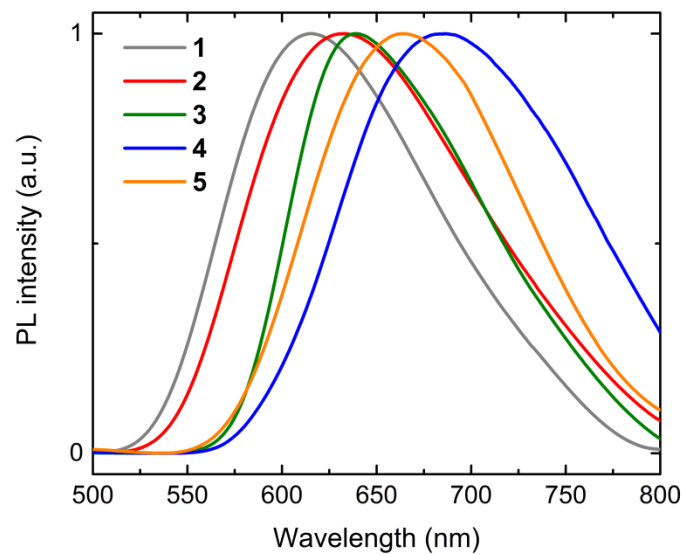


Figure S10. Left: emission spectra of degassed solution of **1-5**; right: emission spectra and the photo of degassed and aerated solution of **1** (1,2-dichloroethane solution, r.t.), $\lambda_{\text{exct}} = 365 \text{ nm}$.¹

¹ The spectra were recorded on Avantes AvaSpec spectrometer.



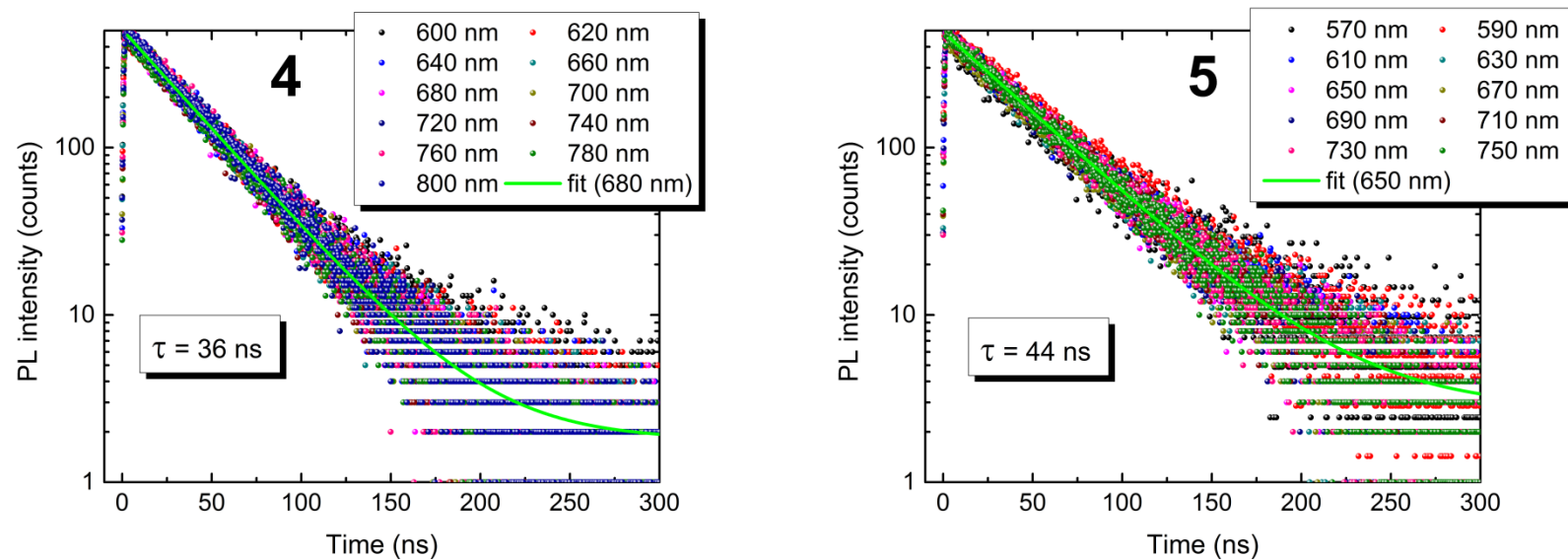


Figure S11. Low energy part of **1-5** emission spectra (**PH** band) for time-resolved experiments and relaxation curves for different wavelengths (1,2-dichloroethane, r.t., $\lambda_{\text{exct}} = 375$ nm). The afterglow time is indicated on diagram.

Table S2. Photophysical properties of the complexes **1-5** in the solid state at variable temperature (oxygen free atmosphere, $\lambda_{\text{exct}} = 375$ nm).

Complex	T	λ_{em} , nm	* τ_1, τ_2, τ_3 , ns	$\langle\tau\rangle$, ns
1	RT	590	272(0.54), 648(0.46)	581
	77 K	577	2110(1.00)	2110
2	RT	563	83(0.55), 356(0.45)	295
	77 K	592	181(0.23), 1498(0.77)	1452
3	RT	650	58(0.49), 255(0.51)	220
	77 K	646	177(0.25), 1593(0.75)	1542
4	RT	677	10(0.39), 41(0.45), 140(0.16)	88
	77 K	663	59(0.53), 344(0.47)	298
5	RT	635	49(0.96), 218(0.04)	75
	77 K	645	135(0.52), 451(0.48)	373

* Contribution of an exponential function with corresponding lifetime to overall PL decay is given in parentheses.

Table S3. Summary of emission energy maxima for **1-5** in different media.

Complex	DCE solution, r.t.	Solid state, r.t.	Solid state, 77 K
1	613	590	577
2	629	563	592
3	640	650	646
4	685	677	663
5	662	635	645

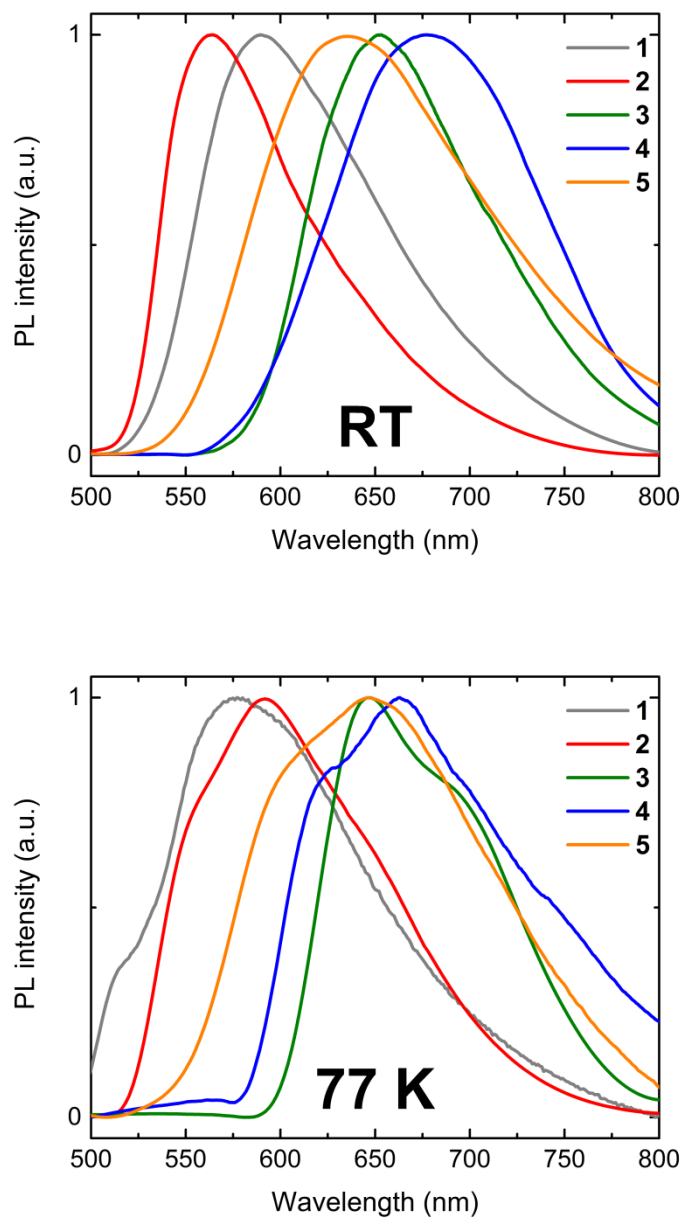
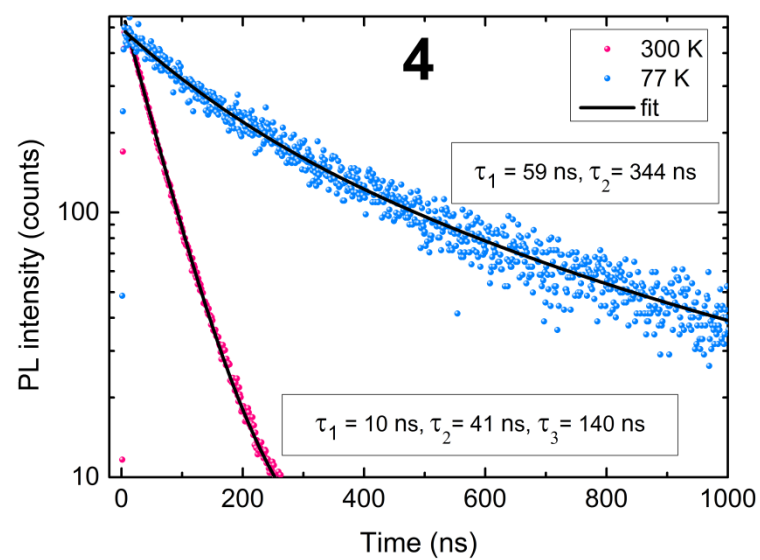
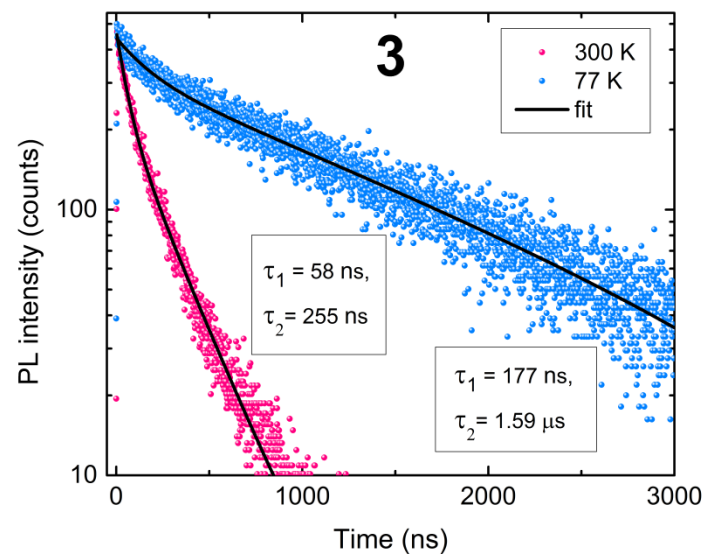
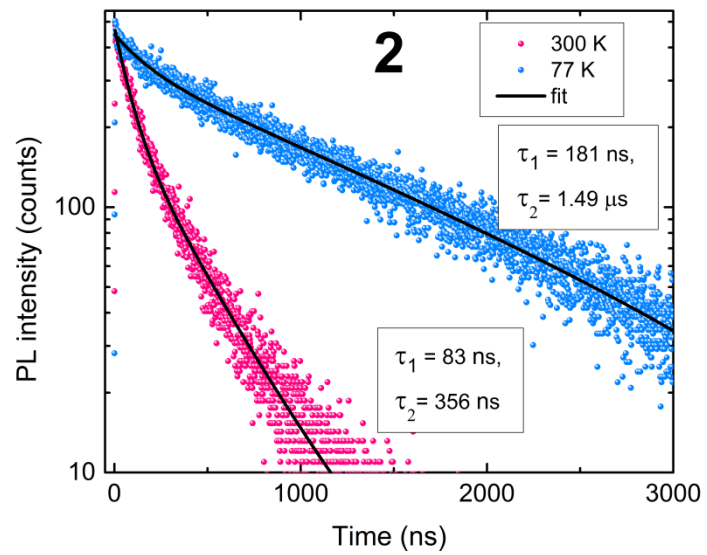
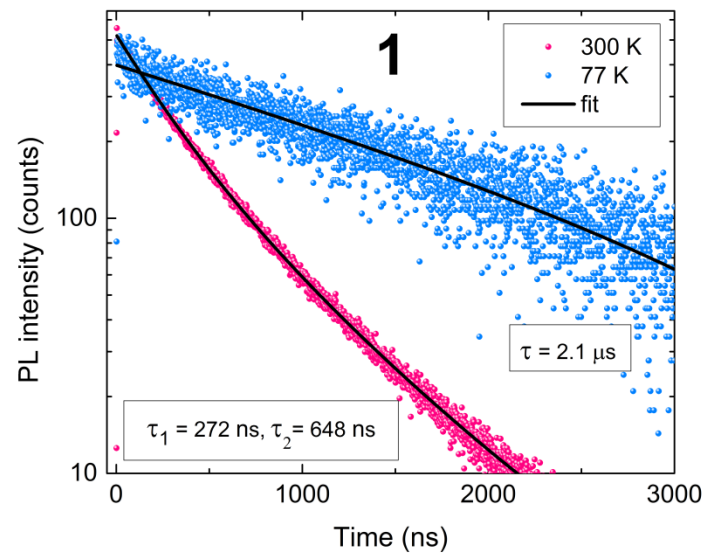


Figure S12. Solid state emission spectra of **1-5** at 298 and 77 K (oxygen free atmosphere, $\lambda_{\text{exct}} = 375$ nm).



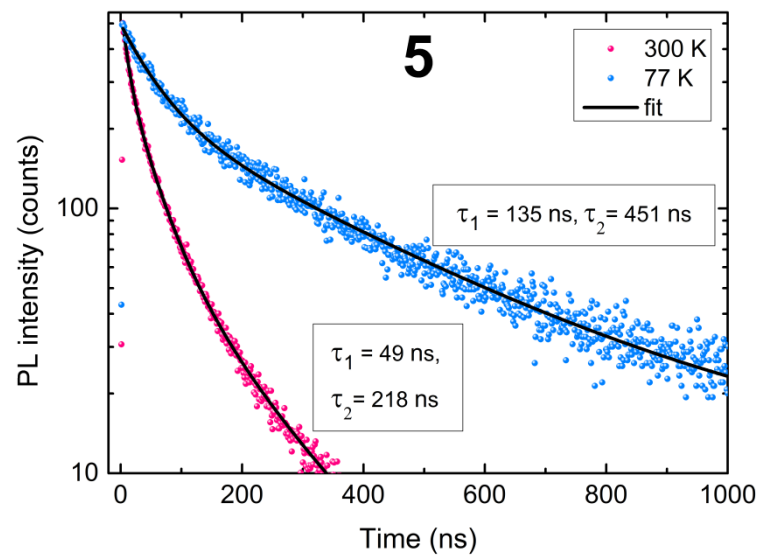


Figure S13. Solid state relaxation curves of **PH** band for **1-5** at variable temperature (oxygen free atmosphere, $\lambda_{\text{exct}} = 375$ nm).

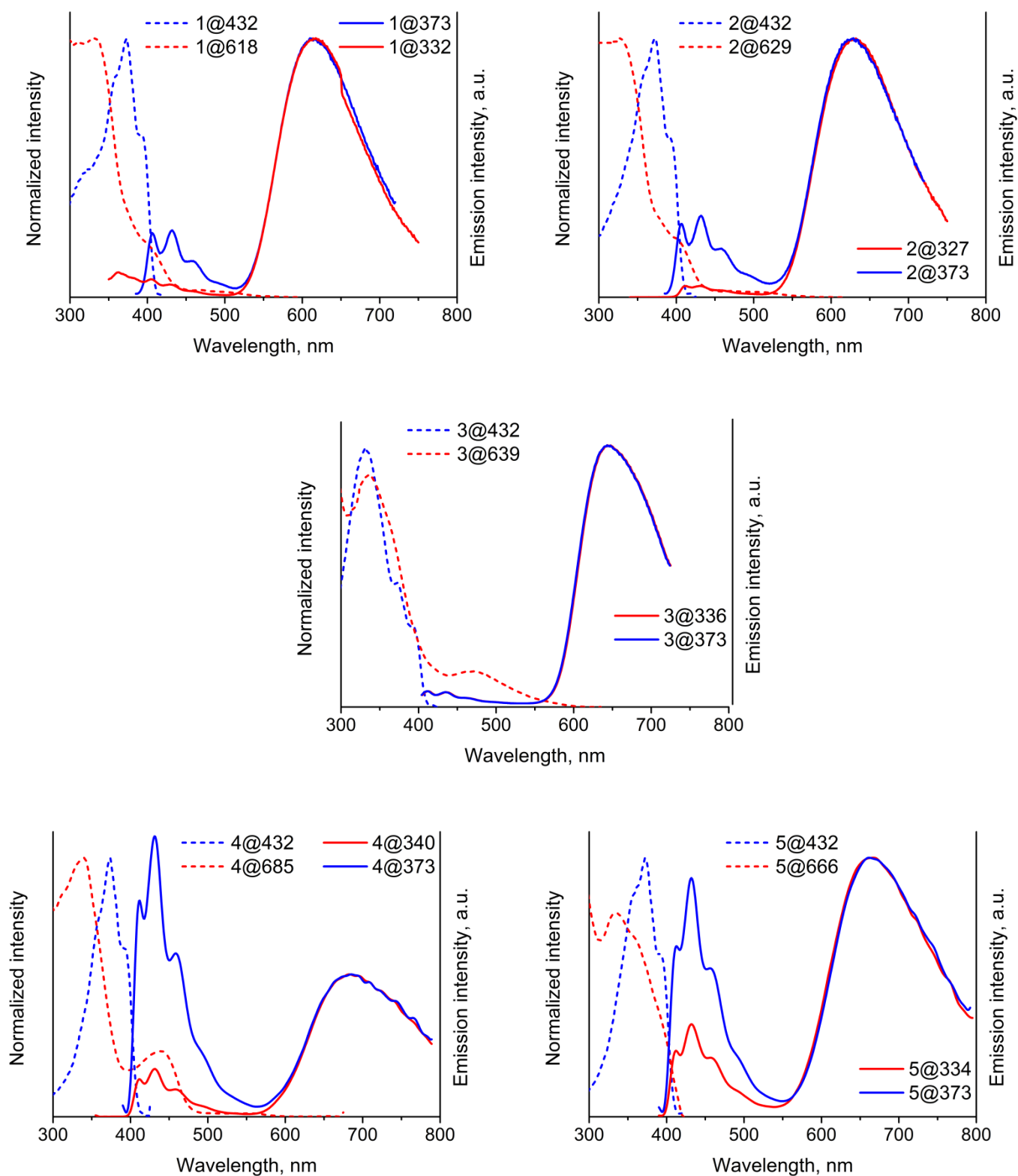


Figure S14. Normalized excitation (dot line) and normalized on **PH** band emission (solid line) spectra of **1-5**, (1,2-dichloroethane, aerated solution, r.t.). Registration and excitation wavelengths are indicated on the diagram.

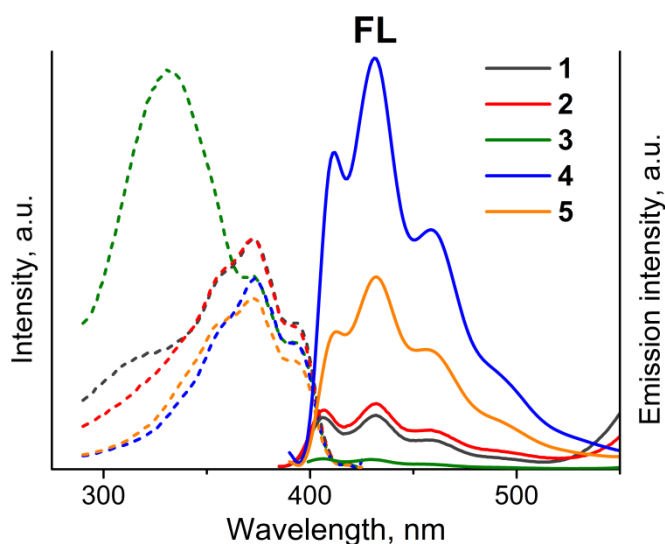


Figure S15. FL excitation (dash line, $\lambda_{\text{em}} = 432$ nm) and FL part (solid line, $\lambda_{\text{exc}} = 375$ nm) of emission spectra of **1-5**, normalized on phosphorescence band (1,2-dichloroethane, aerated solution, r.t.). PH band is out of diagram, the whole emission spectra of **1-5** in 1,2-dichloroethane are shown in Figs. 5 and S14.

Computational results

Selection of computational methodology

Computational methodology was assimilated by benchmark of DFT functionals and basis sets. Pure TPSS¹ and PBE² functionals, TPSSh^{1,3}, PBE0⁴ and B3LYP⁵⁻⁷ hybrids, as well as the long-range-corrected CAM-B3LYP⁸ functional were used in combination with 6-31G* basis set to calculate absorption spectra of the complexes studied in this work. The results have shown that both pure functionals produced a large red shift (50-120 nm) of the primary absorption bands (Fig. S16), while PBE0 and CAM-B3LYP hybrid functionals exhibited significant blue shifts up to 80 nm (Fig. S17). The most reliable behavior among all mentioned functionals was demonstrated by B3LYP, which was therefore chosen for production calculations. Extension of the basis set from double-zeta to triple-zeta quality has a negligible effect on the vertical excitation energies, as well as the account for spin-orbit terms via Douglas-Kroll-Hess 4th order relativistic calculation (DKHSO keyword in Gaussian 09).⁹

- 1 J. Tao, J. P. Perdew, V. N. Staroverov and G. E. Scuseria, *Phys. Rev. Lett.*, 2003, **91**, 146401.
- 2 J. P. Perdew, K. Burke and M. Ernzerhof, *Phys. Rev. Lett.*, 1997, **78**, 1396.
- 3 V. N. Staroverov, G. E. Scuseria, J. Tao and J. P. Perdew, *J. Chem. Phys.*, 2003, **119**, 12129–12137.
- 4 C. Adamo and V. Barone, *J. Chem. Phys.*, 1999, **110**, 6158–6170.
- 5 A. D. Becke, *J. Chem. Phys.*, 1993, **98**, 5648–5652.
- 6 C. Lee, W. Yang and R. G. Parr, *Phys. Rev. B*, 1988, **37**, 785–789.
- 7 P. J. Stephens, F. J. Devlin, C. F. Chabalowski and M. J. Frisch, *J. Phys. Chem.*, 1994, **98**,

11623–11627.

- 8 T. Yanai, D. P. Tew and N. C. Handy, *Chem. Phys. Lett.*, 2004, **393**, 51–57.
- 9 M. J. Frisch, G. W. Trucks, H. B. Schlegel, G. E. Scuseria, M. A. Robb, J. R. Cheeseman, G. Scalmani, V. Barone, B. Mennucci, G. A. Petersson, H. Nakatsuji, M. Caricato, X. Li, H. P. Hratchian, A. F. Izmaylov, J. Bloino, G. Zheng, J. L. Sonnenberg, M. Hada, M. Ehara, K. Toyota, R. Fukuda, J. Hasegawa, M. Ishida, T. Nakajima, Y. Honda, O. Kitao, H. Nakai, T. Vreven, J. A. J. Montgomery, J. E. Peralta, F. Ogliaro, M. Bearpark, J. J. Heyd, E. Brothers, K. N. Kudin, V. N. Staroverov, T. Keith, R. Kobayashi, J. Normand, K. Raghavachari, A. Rendell, J. C. Burant, S. S. Iyengar, J. Tomasi, M. Cossi, N. Rega, J. M. Millam, M. Klene, J. E. Knox, J. B. Cross, V. Bakken, C. Adamo, J. Jaramillo, R. Gomperts, R. E. Stratmann, O. Yazyev, A. J. Austin, R. Cammi, C. Pomelli, J. W. Ochterski, R. L. Martin, K. Morokuma, V. G. Zakrzewski, G. A. Voth, P. Salvador, J. Dannenberg J., S. Dapprich, A. D. Daniels, O. Farkas, J. B. Foresman, J. V. Ortiz, J. Cioslowski and D. J. Fox, *Gaussian 09, Revis. D.01, Gaussian, Inc. 2013*, 2013.

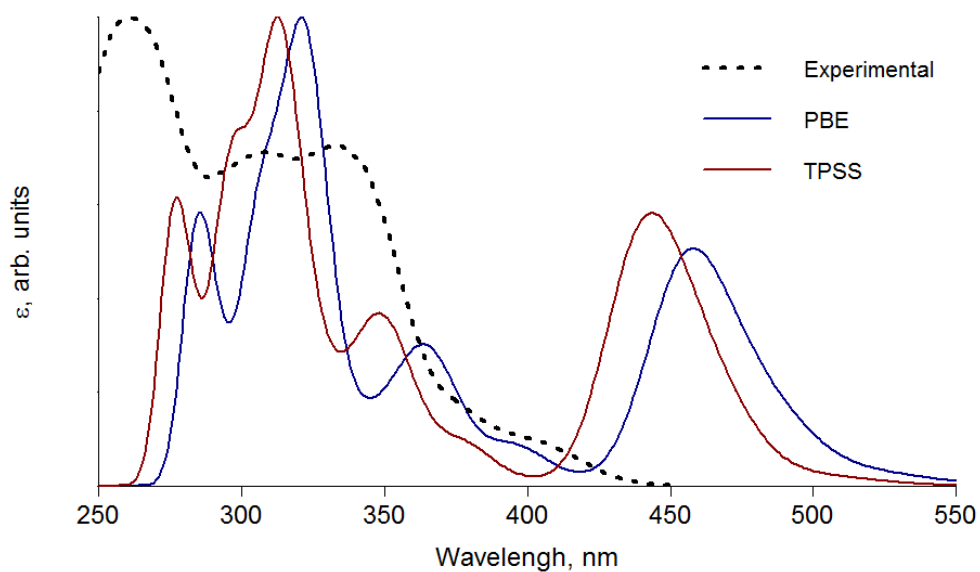


Figure S16. Comparison of pure DFT functionals PBE and TPSS with SDD basis set for iridium atoms and 6-31G* basis set for all other atoms.

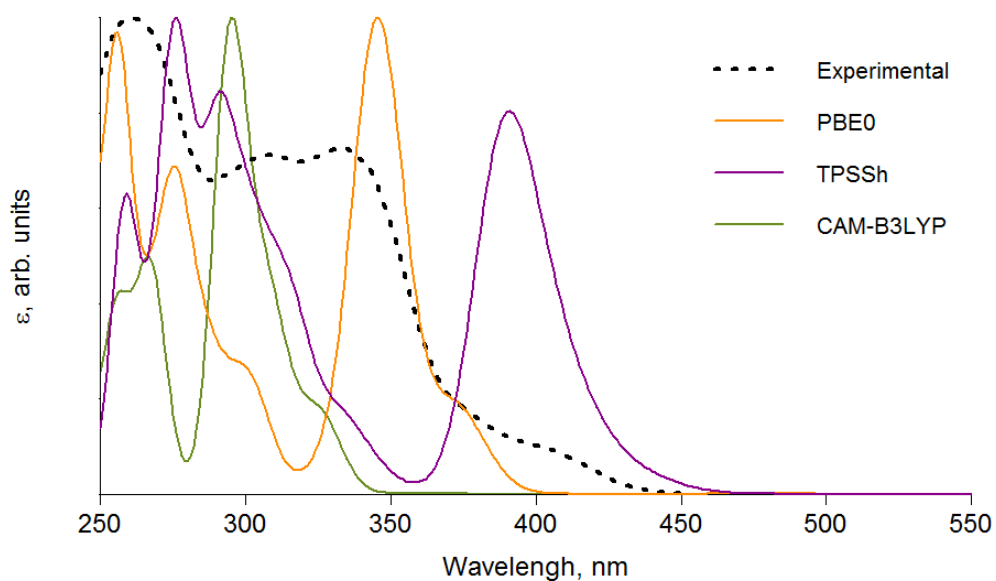


Figure S17. Comparison of hybrid DFT functionals PBE0, TPSSh and CAM-B3LYP with SDD basis set for iridium atoms and 6-31G* basis set for all other atoms.

Table S4. Experimental (**1-3** only) and computed (B3LYP functional together with SDD basis set for iridium atoms and 6-31G* basis set for all other atoms) bonds length (Å) and angles (°) of **1-5**.

	1		2		3	
	Exp	Calcd	Exp	Calcd	Exp	Calcd
Ir-N1	2.068(6)	2.0887	2.059(5)	2.0900	2.092(6)	2.1361
Ir-N2	2.063(6)	2.0900	2.046(4)	2.0907	2.086(6)	2.1380
Ir-N3	2.130(5)	2.2109	2.127(6)	2.2096	2.160(5)	2.2516
Ir-N4	2.137(5)	2.2122	2.133(6)	2.2123	2.170(4)	2.2561
Ir-C31	2.011(7)	2.0307	2.029(6)	2.0319	2.012(6)	2.0178
Ir-C34	2.034(7)	2.0307	1.979(8)	2.0309	2.019(6)	2.0168
N1-Ir1-N2	173.8(2)	176.77	172.6(2)	176.86	171.0(2)	176.01
C34-Ir1-N4	175.4(2)	176.08	175.5(2)	176.40	172.1(2)	174.89
C31-Ir1-N3	172.6(3)	176.40	169.7(3)	176.33	169.4(2)	174.96
C31-Ir1-C34	88.2(3)	89.17	89.8(3)	89.18	88.9(3)	89.98

	4	5
Ir-N1	2.1033	2.1010
Ir-N2	2.1029	2.0991
Ir-N3	2.1890	2.1890
Ir-N4	2.1914	2.1924
Ir-C31	2.0464	2.0035
Ir-C34	2.0457	2.0027
N1-Ir1-N2	179.10	176.34
C34-Ir1-N4	175.95	175.73
C31-Ir1-N3	175.65	175.62
C31-Ir1-C34	89.96	90.24

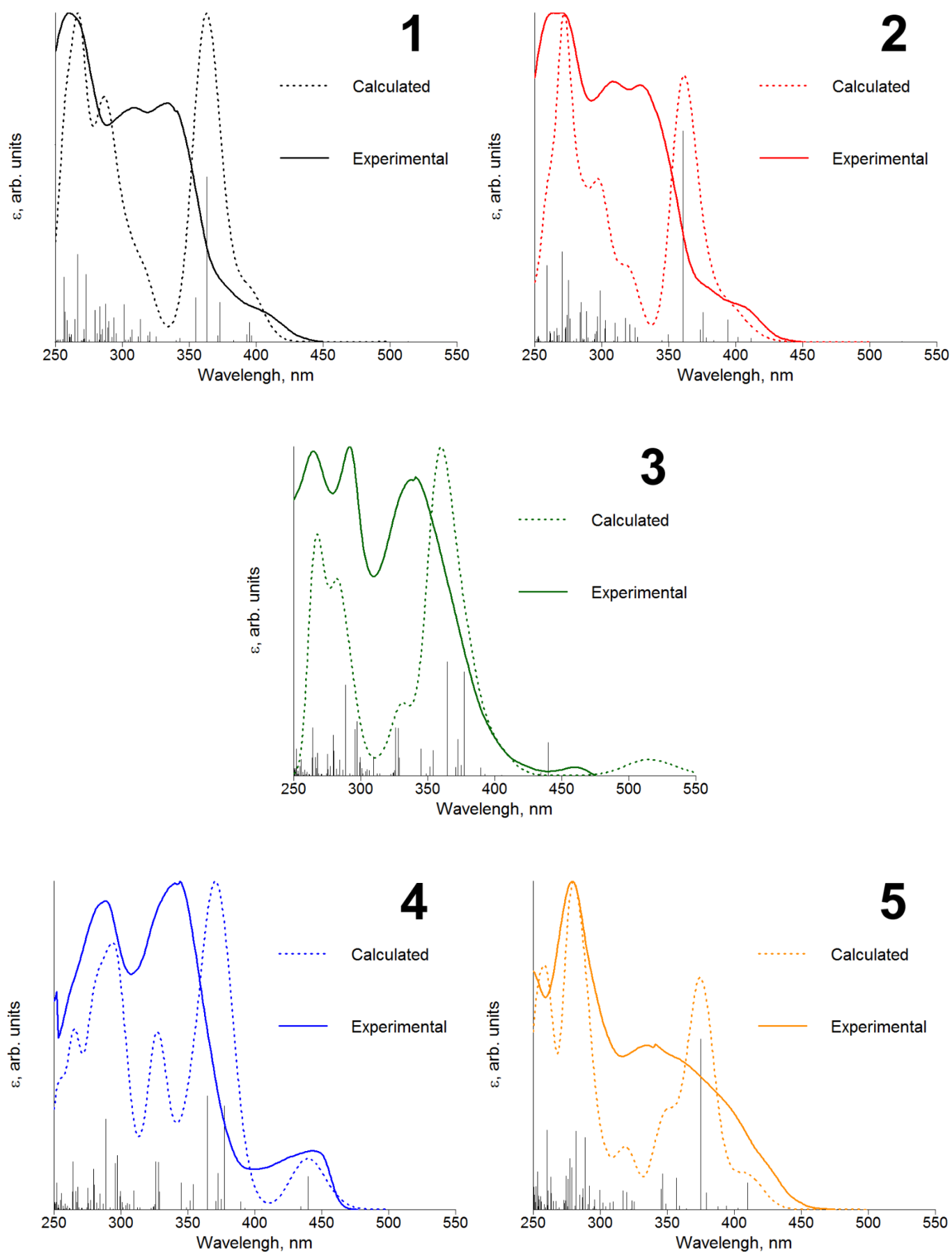


Figure S18. Computed and experimental UV-vis spectra of **1-5** in 1,2-dichloroethane solution (B3LYP functional together with SDD basis set for iridium atoms and 6-31G* basis set for all other atoms).

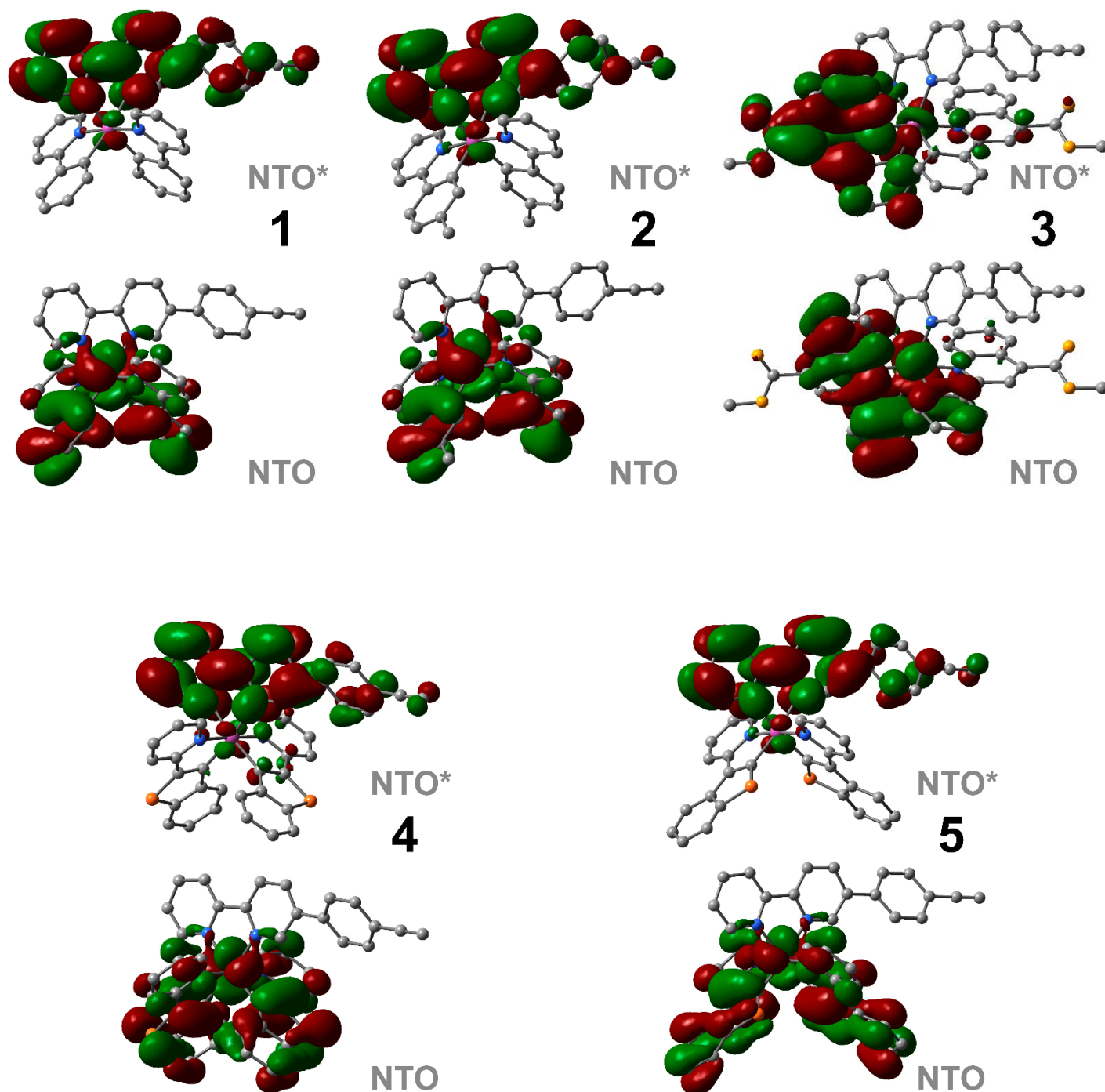


Figure S19. Visualization of triplet transitions in 1-5 by NTO.

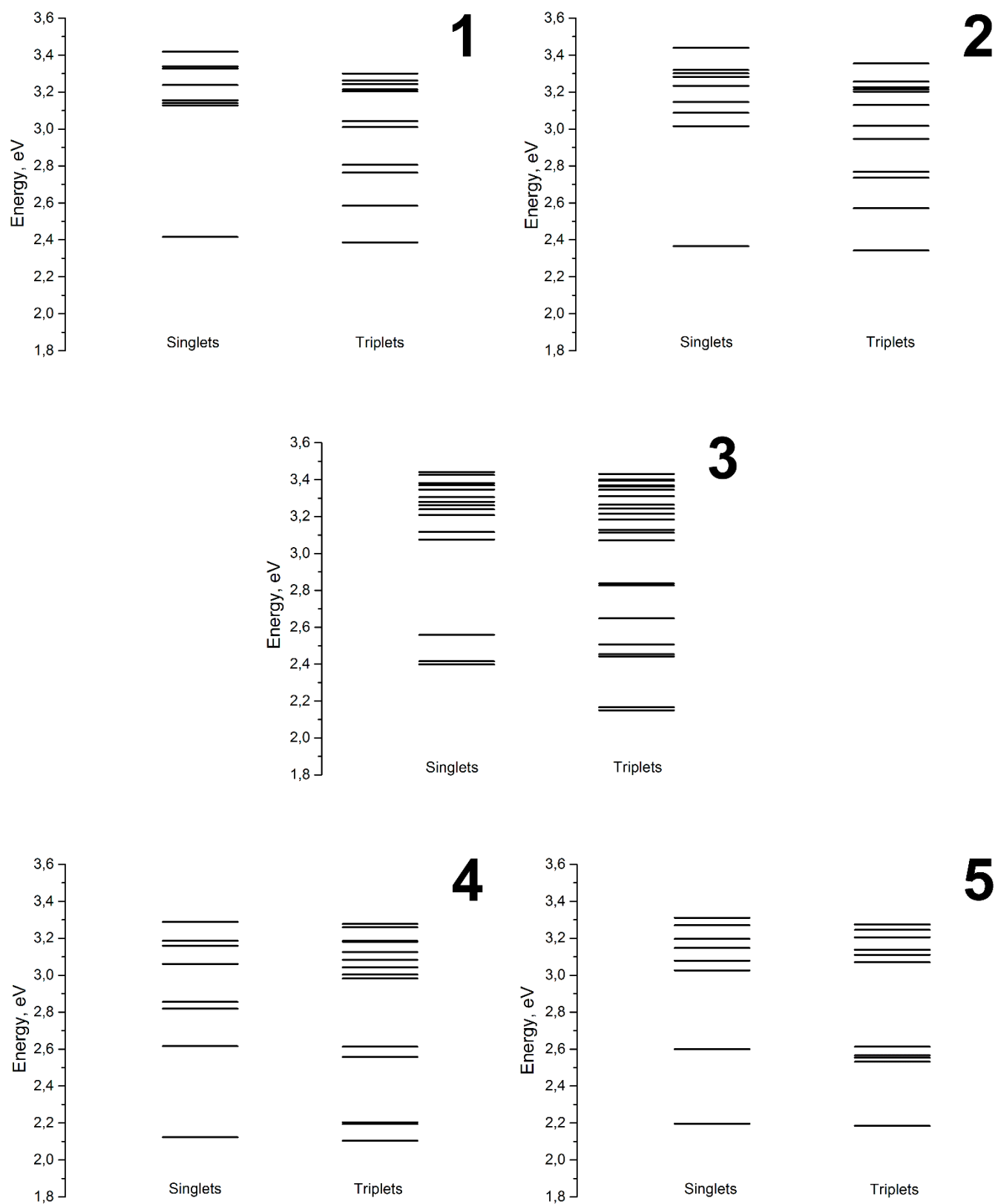


Figure S20. Energies of low-lying singlet and triplet excited states obtained from TDDFT calculations for 1-5.

Table S5. Natural Transition Orbital analysis of electronic excited states in **1-5**.

Complex 1						
State	λ , nm	f	Fragment	Orbital composition		Transition character
				NTO	NTO*	
S ₂	396	0.0183	Ir	0.69		ML'CT
			C^N(1)	0.10		LL'CT
			C^N(2)	0.13		
			NN		0.97	
S ₃	395	0.0581	Ir	0.46		MLCT
			C^N(1)	0.26	0.51	IL
			C^N(2)	0.26	0.41	
			NN			
S ₄	393	0.0223	Ir	0.21		ML'CT
			C^N(1)	0.41		LL'CT
			C^N(2)	0.36		
			NN		0.97	
S ₆	373	0.1198	Ir	0.40		ML'CT
			C^N(1)	0.19		LL'CT
			C^N(2)	0.22		
			NN	0.19	0.97	IL'
S ₈	363	0.5016	Ir			
			C^N(1)	0.11		LL'CT
			C^N(2)	0.13		
			NN (ethynylphenyl)	0.51	0.11	IL'
			NN (bipyridine)	0.19	0.86	
S ₉	355	0.1343	Ir	0.10		ML'CT
			C^N(1)	0.38		LL'CT
			C^N(2)	0.33		
			NN	0.18	0.97	IL'
S ₁₆	313	0.0687	Ir	0.30		ML'CT
			C^N(1)	0.33		LL'CT
			C^N(2)	0.34		
			NN		0.97	
S ₂₂	301	0.1137	Ir	0.34		ML'CT
			C^N(1)	0.31	0.44	LL'CT
			C^N(2)	0.30	0.48	
			NN			
S ₂₄	294	0.0730	Ir	0.46		MLCT
			C^N(1)	0.26	0.51	IL
			C^N(2)	0.26	0.41	
			NN			
S ₂₉	287	0.1145	Ir	0.48		ML'CT
			C^N(1)	0.22		LL'CT
			C^N(2)	0.24		
			NN		0.98	
S ₃₃	283	0.1073	Ir			
			C^N(1)		0.32	IL, LL'CT
			C^N(2)	0.59	0.35	
			NN	0.35	0.28	IL', LL'CT

S ₃₆	279	0.0956	Ir	0.16		ML'CT
			C^N(1)	0.38		LL'CT
			C^N(2)	0.43		
			NN		0.88	
S ₃₈	273	0.2042	Ir	0.45		ML'CT
			C^N(1)	0.22		LL'CT
			C^N(2)	0.23		
			NN		0.95	
S ₄₅	266	0.2654	Ir	0.19		ML'CT, MLCT
			C^N(1)	0.33		IL
			C^N(2)	0.45	0.79	
			NN		0.10	LL'CT
S ₅₅	256	0.1973	Ir			LL'CT
			C^N(1)	0.55		
			C^N(2)	0.37		
			NN		0.86	

Complex 2

State	λ , nm	f	Fragment	Orbital composition		Transition character
				NTO	NTO*	
S ₂	411	0.0113	Ir			L'LCT
			C^N(1)	0.45		
			C^N(2)	0.44		
			NN		0.97	
S ₃	402	0.0144	Ir	0.64		ML'CT
			C^N(1)	0.15		LL'CT
			C^N(2)	0.14		
			NN		0.97	
S ₄	394	0.0662	Ir	0.44		MLCT
			C^N(1)	0.27	0.47	IL
			C^N(2)	0.27	0.46	
			NN			
S ₆	378	0.0129	Ir	0.42		ML'CT
			C^N(1)	0.30		LL'CT
			C^N(2)	0.27		
			NN		0.90	
S ₇	375	0.0896	Ir	0.53		ML'CT
			C^N(1)	0.19		LL'CT
			C^N(2)	0.18		
			NN	0.10	0.97	IL'
S ₈	373	0.0363	Ir	0.19		ML'CT
			C^N(1)	0.36		LL'CT
			C^N(2)	0.37		
			NN		0.97	
S ₉	360	0.6412	Ir			IL'
			C^N(1)			
			C^N(2)			
			NN (ethynylphenyl)	0.66	0.12	
			NN (bipyridine)	0.20	0.86	

S ₁₀	349	0.0223	Ir	0.10		ML'CT
			C^N(1)	0.41		LL'CT
			C^N(2)	0.44		
			NN		0.97	
S ₁₃	325	0.0428	Ir	0.16		MLCT
			C^N(1)	0.41	0.47	IL
			C^N(2)	0.41	0.43	
			NN			
S ₁₅	321	0.0523	Ir	0.31		MLCT
			C^N(1)	0.32	0.49	IL
			C^N(2)	0.34	0.40	
			NN			
S ₁₆	318	0.0711	Ir	0.65		MLCT
			C^N(1)	0.15	0.49	IL
			C^N(2)	0.14	0.40	
			NN			
S ₁₈	312	0.0149	Ir	0.66		MLCT
			C^N(1)	0.15	0.45	IL
			C^N(2)	0.14	0.46	
			NN			
S ₁₉	310	0.0568	Ir	0.57		ML'CT
			C^N(1)	0.14		LL'CT
			C^N(2)	0.15		
			NN	0.15	0.89	IL'
S ₂₃	299	0.1549	Ir	0.21		MLCT, ML'CT
			C^N(1)	0.29	0.13	IL, LL'CT
			C^N(2)	0.33	0.49	
			NN	0.17	0.13	IL, L'LCT
S ₂₄	297	0.0768	Ir	0.15		MLCT, ML'CT
			C^N(1)	0.41	0.70	IL
			C^N(2)	0.34		
			NN	0.10	0.18	IL'
S ₃₀	288	0.0922	Ir	0.12		ML'CT
			C^N(1)	0.11		LL'CT
			C^N(2)			
			NN	0.70	0.97	IL'
S ₃₄	285	0.1202	Ir	0.28		ML'CT
			C^N(1)	0.15		LL'CT
			C^N(2)	0.20		
			NN	0.37	0.97	IL'
S ₃₉	275	0.1871	Ir	0.57		ML'CT
			C^N(1)	0.18		LL'CT
			C^N(2)	0.17		
			NN		0.96	
S ₄₃	270	0.2730	Ir	0.16		ML'CT, MLCT
			C^N(1)			
			C^N(2)		0.13	
			NN	0.69	0.79	IL', L'LCT
S ₅₆	259	0.2324	Ir	0.52	0.34	MLCT, ML'CT
			C^N(1)	0.23	0.28	IL, LL'CT
			C^N(2)	0.23	0.26	
			NN		0.12	

Complex 3

State	λ , nm	f	Fragment	Orbital composition		Transition character
				NTO	NTO*	
S ₄	403	0.0485	Ir	0.37		MLCT
			C [^] N(1)	0.26	0.28	IL
			C [^] N(2)	0.32	0.66	
			NN			
S ₅	398	0.0236	Ir	0.33		MLCT
			C [^] N(1)	0.34	0.27	IL
			C [^] N(2)	0.29	0.69	
			NN			
S ₁₀	375	0.1840	Ir	0.21		MLCT
			C [^] N(1)	0.39	0.56	IL
			C [^] N(2)	0.37	0.39	
			NN			
S ₁₅	360	0.4748	Ir			
			C [^] N(1)			
			C [^] N(2)			
			NN (ethynylphenyl)	0.70	0.12	IL'
			NN (bipyridine)	0.23	0.85	
S ₁₇	354	0.2329	Ir	0.10		MLCT
			C [^] N(1)	0.31	0.38	IL
			C [^] N(2)	0.55	0.57	
			NN			
S ₂₆	330	0.1708	Ir	0.42		MLCT, ML'CT
			C [^] N(1)	0.28	0.56	IL, LL'CT
			C [^] N(2)	0.28	0.33	
			NN		0.10	
S ₃₇	295	0.0620	Ir	0.17		ML'CT
			C [^] N(1)			LL'CT
			C [^] N(2)	0.13		
			NN	0.62	0.89	IL'
S ₄₃	289	0.0855	Ir	0.34		MLCT, ML'CT
			C [^] N(1)	0.28	0.11	LL'CT, IL
			C [^] N(2)	0.33	0.26	
			NN		0.59	
S ₄₆	284	0.1878	Ir			
			C [^] N(1)			
			C [^] N(2)			
			NN	0.97	0.89	IL'
S ₄₇	282	0.1029	Ir	0.37		ML'CT
			C [^] N(1)	0.28		LL'CT
			C [^] N(2)	0.30		
			NN		0.94	
S ₄₈	280	0.1262	Ir	0.22		ML'CT, MLCT
			C [^] N(1)	0.49		IL, LL'CT
			C [^] N(2)	0.21	0.15	
			NN		0.82	
S ₅₅	272	0.1053	Ir	0.37		MLCT, ML'CT
			C [^] N(1)	0.34	0.35	IL, LL'CT
			C [^] N(2)	0.18	0.19	
			NN	0.11	0.38	IL'

S ₆₆	266	0.1528	Ir	0.13		MLCT
			C^N(1)	0.50		IL
			C^N(2)	0.21	0.85	
			NN	0.16		LL'CT

Complex 4

State	λ , nm	f	Fragment	Orbital composition		Transition character
				NTO	NTO*	
S ₃	440	0.1006	Ir	0.28		MLCT
			C^N(1)	0.34	0.58	IL
			C^N(2)	0.37	0.33	
			NN			
S ₄	434	0.0089	Ir	0.26		MLCT
			C^N(1)	0.37	0.59	IL
			C^N(2)	0.35	0.33	
			NN			
S ₈	377	0.3152	Ir	0.41		ML'CT
			C^N(1)	0.10		LL'CT
			C^N(2)	0.11		
			NN (ethynylphenyl)	0.35		IL'
			NN (bipyridine)	0.16	0.98	
S ₁₀	373	0.1094	Ir			
			C^N(1)	0.47	0.24	IL
			C^N(2)	0.51	0.67	
			NN			
S ₁₂	364	0.3451	Ir	0.35		ML'CT
			C^N(1)	0.13		LL'CT
			C^N(2)			
			NN	0.46	0.97	IL'
S ₁₃	354	0.0769	Ir	0.59		ML'CT
			C^N(1)	0.12		LL'CT
			C^N(2)	0.16		
			NN	0.13	0.97	IL'
S ₁₆	345	0.0808	Ir	0.24		MLCT, ML'CT
			C^N(1)	0.37	0.38	IL, LL'CT
			C^N(2)	0.37	0.48	
			NN		0.12	
S ₁₈	328	0.1437	Ir	0.21		MLCT
			C^N(1)	0.40	0.49	IL
			C^N(2)	0.37	0.41	
			NN			
S ₁₉	326	0.1447	Ir			
			C^N(1)	0.27	0.34	IL
			C^N(2)	0.64	0.59	
			NN			
S ₂₆	309	0.0572	Ir			
			C^N(1)	0.43	0.70	IL
			C^N(2)	0.53	0.25	
			NN			

S ₃₄	297	0.1641	Ir	0.49		MLCT
			C^N(1)	0.19	0.78	IL
			C^N(2)		0.13	
			NN	0.27		L'LCT
S ₃₅	295	0.1402	Ir	0.25		MLCT
			C^N(1)			IL
			C^N(2)	0.10	0.92	
			NN	0.62		L'LCT
S ₃₈	288	0.2748	Ir			
			C^N(1)			
			C^N(2)			
			NN	0.97	0.95	IL'
S ₄₅	279	0.1228	Ir	0.31		MLCT
			C^N(1)	0.33		IL
			C^N(2)	0.34	0.83	
			NN			
S ₅₈	264	0.1452	Ir	0.61		ML'CT
			C^N(1)	0.11		LL'CT
			C^N(2)	0.19		
			NN		0.95	
S ₇₆	252	0.0817	Ir	0.38		ML'CT, MLCT
			C^N(1)		0.23	
			C^N(2)		0.55	
			NN	0.47	0.19	IL', L'LCT

Complex 5

State	λ , nm	f	Fragment	Orbital composition		Transition character
				NTO	NTO*	
S ₃	410	0.0810	Ir	0.28		MLCT
			C^N(1)	0.23	0.41	IL
			C^N(2)	0.38	0.42	
			NN			
S ₄	403	0.0039	Ir			
			C^N(1)	0.42		LL'CT
			C^N(2)	0.47		
			NN		0.97	
S ₇	379	0.0501	Ir			
			C^N(1)	0.49		LL'CT
			C^N(2)	0.40		
			NN		0.97	
S ₈	374	0.5184	Ir	0.10		ML'CT
			C^N(1)			
			C^N(2)			
			NN (ethynylphenyl)	0.58	0.10	IL'
			NN (bipyridine)	0.21	0.87	
S ₁₁	357	0.0963	Ir	0.63		ML'CT
			C^N(1)			
			C^N(2)			
			NN	0.18	0.97	IL'

S ₁₃	346	0.1088	Ir	0.65		ML'CT
			C^N(1)	0.13		LL'CT
			C^N(2)	0.11		
			NN	0.12	0.97	IL'
S ₁₄	345	0.0614	Ir			IL, LL'CT
			C^N(1)	0.52	0.41	
			C^N(2)	0.46	0.13	
			NN		0.40	
S ₁₈	319	0.0517	Ir			IL
			C^N(1)	0.46	0.43	
			C^N(2)	0.45	0.43	
			NN			
S ₁₉	317	0.0567	Ir	0.19		MLCT, ML'CT
			C^N(1)	0.39	0.31	IL, LL'CT
			C^N(2)	0.41	0.28	
			NN		0.38	
S ₂₆	299	0.0579	Ir	0.12		MLCT, ML'CT
			C^N(1)		0.11	
			C^N(2)			
			NN	0.84	0.79	IL', L'LCT
S ₃₄	288	0.2195	Ir			
			C^N(1)			
			C^N(2)			
			NN	0.99	0.97	
S ₃₈	282	0.2382	Ir	0.22	0.12	MC, MLCT
			C^N(1)	0.38	0.39	IL
			C^N(2)	0.39	0.44	
			NN			
S ₄₀	277	0.1274	Ir	0.60	0.35	MC, ML'CT
			C^N(1)	0.13		
			C^N(2)			
			NN	0.21	0.51	IL'
S ₄₁	277	0.1544	Ir	0.61		MLCT, ML'CT
			C^N(1)			IL, LL'CT
			C^N(2)	0.14	0.20	
			NN	0.16	0.66	IL', L'LCT
S ₄₅	274	0.1025	Ir	0.10		ML'CT
			C^N(1)			
			C^N(2)			
			NN	0.86	0.94	IL'
S ₅₄	263	0.0980	Ir	0.62		ML'CT
			C^N(1)			LL'CT
			C^N(2)	0.13		
			N^N	0.15	0.90	IL'
S ₅₇	260	0.2417	Ir	0.65		ML'CT
			C^N(1)	0.15		LL'CT
			C^N(2)			
			N^N	0.12	0.96	IL
S ₆₆	253	0.1143	Ir			LL'CT
			C^N(1)	0.58		
			C^N(2)	0.36		
			N^N		0.80	